

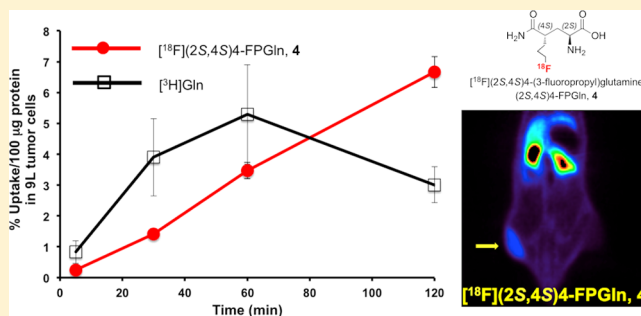
[¹⁸F](2S,4S)-4-(3-Fluoropropyl)glutamine as a Tumor Imaging Agent

Zehui Wu,^{†,§} Zhihao Zha,^{†,§} Genxun Li,[†] Brian P. Lieberman,[†] Seok Rye Choi,[†] Karl Ploessl,[†] and Hank F. Kung^{*,†,‡}

[†]Departments of Radiology and [‡]Pharmacology, University of Pennsylvania, 3700 Market Street, Philadelphia, Pennsylvania 19104, United States

ABSTRACT: Although the growth and proliferation of most tumors is fueled by glucose, some tumors are more likely to metabolize glutamine. In particular, tumor cells with the upregulated c-Myc gene are generally reprogrammed to utilize glutamine. We have developed new 3-fluoropropyl analogs of glutamine, namely [¹⁸F](2S,4R)- and [¹⁸F](2S,4S)-4-(3-fluoropropyl)glutamine, 3 and 4, to be used as probes for studying glutamine metabolism in these tumor cells. Optically pure isomers labeled with ¹⁸F and ¹⁹F (2S,4S) and (2S,4R)-4-(3-fluoropropyl)glutamine were synthesized via different routes and isolated in high radiochemical purity (≥95%). Cell uptake studies of both isomers showed that they were taken up efficiently by 9L tumor cells with a steady increase over a time frame of 120 min. At 120 min, their uptake was approximately two times higher than that of L-[³H]glutamine ([³H]Gln). These in vitro cell uptake studies suggested that the new probes are potential tumor imaging agents. Yet, the lower chemical yield of the precursor for 3, as well as the low radiochemical yield for 3, limits the availability of [¹⁸F](2S,4R)-4-(3-fluoropropyl)glutamine, 3. We, therefore, focused on [¹⁸F](2S,4S)-4-(3-fluoropropyl)glutamine, 4. The in vitro cell uptake studies suggested that the new probe, [¹⁸F](2S,4S)-4-(3-fluoropropyl)glutamine, 4, is most sensitive to the LAT transport system, followed by System N and ASC transporters. A dual-isotope experiment using L-[³H]glutamine and the new probe showed that the uptake of [³H]Gln into 9L cells was highly associated with macromolecules (>90%), whereas the [¹⁸F](2S,4S)-4-(3-fluoropropyl)glutamine, 4, was not (<10%). This suggests a different mechanism of retention. In vivo PET imaging studies demonstrated tumor-specific uptake in rats bearing 9L xenografts with an excellent tumor to muscle ratio (maximum of ~8 at 40 min). [¹⁸F](2S,4S)-4-(3-fluoropropyl)glutamine, 4, may be useful for testing tumors that may metabolize glutamine related amino acids.

KEYWORDS: cancer, metabolism, PET imaging, glutamine and radiolabeling



INTRODUCTION

In the past two decades, the use of 2-[¹⁸F]fluoro-2-deoxy-D-glucose (FDG) and positron emission tomography (PET) has achieved widespread acceptance as an effective tool for detecting cancers with high rates of glycolysis. It is generally accepted that a high rate of glucose metabolism (Warburg effect) is associated with changes in tumor-driven alternative gene expression.^{1,2} However, despite the tremendous promise of FDG-PET for detecting and monitoring tumor metabolism, a significant portion of malignant tumors are not FDG-positive and can be missed in a FDG-PET scan. Accordingly, there is a clear and urgent need to develop additional metabolic tracers, particularly for cancers with low FDG-uptake.

Recent reports suggest that metabolic reprogramming may cause some cancers to switch their energy source from glucose to glutamine.^{3–6} These tumors could be imaged with ¹⁸F-labeled glutamine tracers.^{7–9} Glutamine, which is found circulating in the blood and is also concentrated in the skeletal muscles (0.5–1 mmol/L), has various critical functions: as a substrate for DNA and protein synthesis, a primary source of fuel for cells lining the inside of the small intestine and rapidly dividing immune cells, and as a regulator of acid–base balance

by producing ammonium in the kidneys. Enhanced glutamine utilization in cancers due to changes in the expression of oncogenic signaling pathways can lead to glutaminolysis. In these cases, blocking glutamine synthetic pathways may lead to tumor cell death.¹⁰ Glutamine imaging agents may be useful for testing the therapeutic efficacy of antitumor agents aimed at reducing glutamine metabolism in tumors.

In order to study glutamine metabolizing tumors, we previously prepared and tested L-S-[¹¹C]glutamine.⁷ In tumor cell uptake studies, the maximum uptake of L-S-[¹¹C]glutamine reached 17.9 and 22.5% uptake/100 μg protein at 60 min in 9L and SF188 tumor cells, respectively. At 30 min after incubation, >30% of the activity appeared to be incorporated into cellular proteins. Dynamic small animal PET studies in rats bearing xenografts of 9L tumor and in transgenic mice bearing

Special Issue: Positron Emission Tomography: State of the Art

Received: March 29, 2014

Revised: August 5, 2014

Accepted: August 5, 2014

Published: August 5, 2014

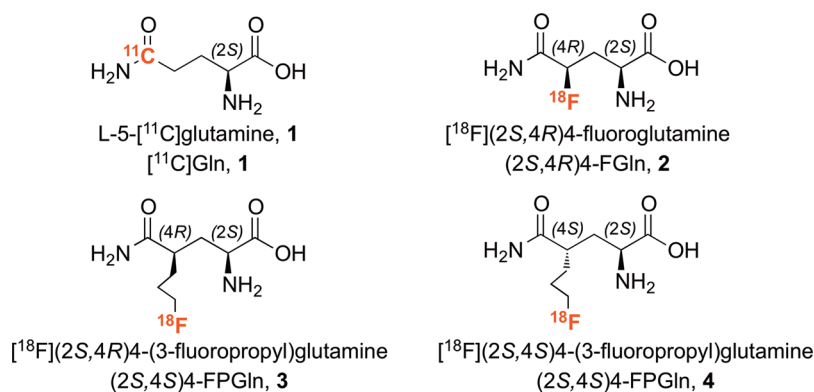


Figure 1. Chemical structures of L-5-¹¹C]glutamine, **1**, (¹¹C]Gln), [¹⁸F](2S,4R)-4-fluoroglutamine, **2** ([¹⁸F](2S,4R)-4-FGln), [¹⁸F](2S,4R)-4-(3-fluoropropyl)glutamines, **3**, ([¹⁸F](2S,4R)-4-FPGln), and [¹⁸F](2S,4S)-4-(3-fluoropropyl)glutamines, **4**, ([¹⁸F](2S,4S)-4-FPGln).

spontaneous mammary gland tumors showed prominent tumor uptake and retention. The results suggested that L-5-¹¹C]-glutamine would be useful for probing in vivo tumor metabolism in glutaminolytic tumors.⁷

Because ¹¹C has a half-life of 20 min, it would not be practical for most clinical settings. To make an imaging agent that would be better for clinical use, we created an alternative metabolic tracer labeled with ¹⁸F, which has a half-life of 110 min. In vitro studies with [¹⁸F](2S,4R)-4-fluoroglutamine, **2** ([¹⁸F](2S,4R)-4-FGln) showed that both 9L and SF188 tumor cells displayed a high rate of glutamine uptake (maximum uptake ≈16% dose/100 μg protein), and the radioactivity trapped inside the cell was associated with the macromolecular fraction precipitated by trichloroacetic acid (TCA). The cell uptake of [¹⁸F](2S,4R)-4-FGln, **2**, by SF188 cells is comparable to that of [³H]L-glutamine but higher than that of FDG. Biodistribution and PET imaging studies showed that [¹⁸F](2S,4R)-4-FGln, **2**, localized in tumors with a higher uptake than that of surrounding muscle and liver tissues, suggesting that [¹⁸F](2S,4R)-4-FGln, **2**, is selectively taken up and trapped by the tumor cells.^{8,9}

One of the drawbacks of [¹⁸F](2S,4R)-4-FGln, **2**, (and its related optical isomers) is the radiolabeling reaction, which is relatively difficult and prone to formation of stereoisomers due to a secondary fluorination reaction.⁹ To avoid this complication, we have designed and tested [¹⁸F](2S,4R)-4-(3-fluoropropyl)glutamine, **3** ([¹⁸F](2S,4R)-4-FPGln), and [¹⁸F](2S,4S)-4-(3-fluoropropyl)glutamine, **4** ([¹⁸F](2S,4S)-4-FPGln), as alternative probes for imaging glutamine metabolism (Figure 1). The 4-(3-fluoropropyl)glutamines contain an extended propyl group. This will make it easier for the S_N2 fluorine substitution with a good leaving group (—OTs) used in the labeling reaction. To preserve the amide functional group at the C5 position, we have synthesized two types of precursors suitable for radiolabeling (fluoro for tosylate substitution reaction). Reported herein is the preparation and in vitro and in vivo studies of these glutamine analogs.

EXPERIMENTAL SECTION

General Information. All reagents used were commercial products and were used without further purification unless otherwise indicated. Boc-Glu(OBzl)—OH (Boc-L-glutamic acid 5-benzyl ester, **15**) was purchased from Sigma-Aldrich. Flash chromatography (FC) was performed using silica gel 60 (230–400 mesh, Sigma-Aldrich). ¹H NMR spectra were obtained at 200 MHz and ¹³C NMR spectra were recorded at 50 MHz

(Bruker DPX 200 spectrometer). Chemical shifts are reported as δ values (parts per million) relative to remaining protons in deuterated solvent. Coupling constants are reported in hertz. The multiplicity is defined by s (singlet), d (doublet), t (triplet), q (quartet), p (pentet), br (broad), or m (multiplet). HPLC analyses were performed on an Agilent LC 1100 series. High-resolution MS experiments were performed using an Agilent Technologies LC/MSD TOF mass spectrometer.

Syntheses. Compounds **5**–**8** were synthesized according to the procedures reported previously.⁹

(*S*)-*tert*-Butyl 2-(*tert*-butoxycarbonylamino)-4-(*tosyloxy*) Butanoate (**9**). To a solution of compound **8** (554 mg, 2 mmol) in 10 mL of dry dichloromethane (DCM) was added Et₃N (1.4 mL, 10 mmol), 4-(dimethylamino)pyridine (DMAP, 24 mg, 0.2 mmol), and *p*-toluenesulfonyl chloride (TsCl, 764 mg, 4 mmol) at 0 °C. The mixture was stirred at room temperature (rt) overnight. Ice-cold water (15 mL) was poured into the reaction mixture and the mixture was extracted with DCM (15 × 3 mL), the combined organic layer was dried with magnesium sulfate (MgSO₄) and was purified with flash chromatography (FC, EtOAc/hexane = 2/8) to give 739.6 mg colorless oil **9** (yield: 86.1%). ¹HNMR (200 MHz, CDCl₃) δ: 1.39–1.54 (m, 18H), 2.08–2.21 (m, 2H), 2.47 (s, 3H), 4.06–4.09 (m, 2H), 4.13–4.16 (m, 1H), 5.03–5.10 (m, 1H), 7.37 (d, *J* = 7.8 Hz, 2H), 7.81 (d, *J* = 8.2 Hz, 2H). HRMS was calcd for C₂₀H₃₂NO₇S (M + H)⁺: 430.1899. Found: 430.1910.

(*S*)-*tert*-Butyl 2-(*tert*-butoxycarbonylamino)-4-cyanobutanoate (**10**). Sodium iodide (240 mg, 1.6 mmol) was added to a solution of compound **9** (343 mg, 0.8 mmol) in 10 mL of acetone (HPLC grade) at rt. The mixture was stirred at 60 °C for 3 h. The solvent was then removed and the residue was dissolved in 15 mL of DCM. The precipitated solid was filtered out and filtrate was concentrated. *N,N*-Dimethylformamide (DMF, 7 mL) and potassium cyanide (78 mg, 1.2 mmol) were added to the residue. The mixture was stirred at rt overnight. The reaction mixture was quenched with 25 mL of ethyl acetate and was washed with H₂O (10 × 3 mL). The organic layer was dried over MgSO₄ and filtered. The filtrate was concentrated, and the residue was purified by FC (EtOAc/hexane = 2/8) to give 196.2 mg colorless oil **10** (yield: 86.3%). ¹HNMR (200 MHz, CDCl₃) δ: 1.39–1.52 (m, 18H), 1.90–2.04 (m, 1H), 2.20–2.30 (m, 1H), 2.40–2.46 (m, 2H), 4.20–4.30 (m, 1H), 5.12–5.22 (m, 1H). HRMS was calcd for C₁₄H₂₅N₂O₄ (M + H)⁺: 302.2080. Found: 302.2078.

(*2S,4S*)-*tert*-Butyl 2-(*tert*-Butoxycarbonylamino)-4-cyanohept-6-enoate (**11a**) and (*2S,4R*)-*tert*-Butyl 2-(*tert*-Butoxy-

carbonylamino)-4-cyanohept-6-enoate (**11b**). LiHMDS (lithium bis(trimethylsilyl)amide) (1.5 mL, 1 mol/L solution in THF) was added to a three-necked 250 mL flask. The mixture was cooled down to -78°C with a dry ice-acetone bath. Compound **10** (201 mg 0.67 mmol) in 3 mL of dry THF solution was added dropwise over 30 min. After being stirred at -78°C for 2 h, allyl bromide (0.24 mL, 2.8 mmol) was added dropwise over 15 min. The mixture was then stirred at -78°C for another 4 h. The reaction was quenched with 20 mL of ethyl acetate and 15 mL of HCl (2 M) and extracted with ethyl acetate (20 \times 3 mL). The organic layer was dried over MgSO_4 and filtered. The filtrate was concentrated, and the residue was purified by FC (EtOAc/hexane = 2/8) to give 60.9 mg **11a** (yield: 28.0%) and 32.6 mg **11b** (yield: 15.1%). **11a**: $^1\text{H NMR}$ (200 MHz, CDCl_3) δ : 1.39–1.52 (m, 18H), 1.90–2.24 (m, 2H), 2.44–2.62 (m, 2H), 2.71–2.85 (m, 1H), 4.35–4.45 (m, 1H), 5.22–5.27 (m, 1H), 5.30–5.36 (m, 2H), 5.70–5.91 (m, 1H). HRMS was calcd for $\text{C}_{17}\text{H}_{29}\text{N}_2\text{O}_4$ ($\text{M} + \text{H}$) $^+$: 325.2127. Found: 325.2125. **11b**: $^1\text{H NMR}$ (200 MHz, CDCl_3) δ : 1.39–1.52 (m, 18H), 1.70–1.90 (m, 1H), 2.05–2.25 (m, 1H), 2.3–2.55 (m, 2H), 2.71–2.85 (m, 1H), 4.35–4.45 (m, 1H), 5.22–5.36 (m, 3H), 5.70–5.91 (m, 1H). HRMS was calcd for $\text{C}_{17}\text{H}_{29}\text{N}_2\text{O}_4$ ($\text{M} + \text{H}$) $^+$: 325.2127. Found: 325.2125.

(2S,4S)-tert-Butyl 2-(tert-Butoxycarbonylamino)-4-cyano-7-hydroxyheptanoate (**12a**) and *(2S,4R)*-tert-Butyl 2-(tert-Butoxycarbonylamino)-4-cyano-7-hydroxyheptanoate (**12b**). To a solution of compound **11a** (91 mg, 0.28 mmol) in 7 mL of THF was added 9-borabicyclo[3.3.1]nonane (9-BBN, 2.22 mL, 0.5 M solution in THF) dropwise at 0°C . After being stirred at 0°C for 1 h, the reaction mixture was moved to rt and stirred for another 48 h. The mixture was then cooled with an ice-bath. H_2O_2 (0.31 mL of 30 wt % solution in H_2O) and NaOH (0.4 mL, 1 M) were added dropwise. The mixture was stirred at rt for 30 min, diluted with 15 mL of H_2O and extracted with ethyl acetate. The organic layer was dried over MgSO_4 and filtered. The filtrate was concentrated, and the residue was purified by FC (EtOAc/hexane = 1/1) to give 30.7 mg colorless oil **12a** (yield: 32.1%). $^1\text{H NMR}$ (200 MHz, CDCl_3) δ : 1.39–1.52 (m, 18H), 1.80–1.95 (m, 4H), 1.96–2.15 (m, 2H), 2.70–2.85 (m, 1H), 3.69–3.75 (m, 2H), 4.20–4.35 (m, 1H), 5.20–5.35 (m, 1H). HRMS was calcd for $\text{C}_{17}\text{H}_{30}\text{N}_2\text{O}_5$ ($\text{M} + \text{H}$) $^+$: 343.2233. Found: 343.2258.

Compound **12b** was prepared from **11b** (194 mg, 0.6 mmol), 9-BBN (4.8 mL, 0.5 M solution in THF), H_2O_2 (0.65 mL of 30 wt % solution in H_2O), and NaOH (0.9 mL, 1 M), following the same procedure described for compound **12a**. Compound **12b**: 91 mg (yield: 44.6%). $^1\text{H NMR}$ (200 MHz, CDCl_3) δ : 1.39–1.52 (m, 18H), 1.70–1.85 (m, 4H), 1.86–2.01 (m, 1H), 2.09–2.30 (m, 1H), 2.70–2.85 (m, 1H), 3.65–3.75 (m, 2H), 4.25–4.40 (m, 1H), 5.10–5.25 (m, 1H). HRMS was calcd for $\text{C}_{17}\text{H}_{30}\text{N}_2\text{O}_5$ ($\text{M} + \text{H}$) $^+$: 343.2233. Found: 343.2258.

(2S,4S)-tert-Butyl 2-(tert-Butoxycarbonylamino)-4-cyano-7-(tosyloxy)heptanoate (**13a**) and *(2S,4R)*-tert-Butyl 2-(tert-Butoxycarbonylamino)-4-cyano-7-(tosyloxy)heptanoate (**13b**). To a solution of compound **12a** (137 mg, 0.4 mmol) in 7 mL of DCM was added Et_3N (0.3 mL, 2.1 mmol) and DMAP (5 mg, 0.04 mmol) at 0°C , followed by TsCl (153 mg, 0.8 mmol). The resulting mixture was stirred at 0°C for 1 and 24 h at rt. The reaction was quenched with 15 mL of water and extracted with DCM (10 \times 3 mL). The organic layer was dried over MgSO_4 and filtered. The filtrate was concentrated, and the residue was purified by FC (EtOAc/hexane = 2/8) to give 180.2 mg of colorless oil **13a** (yield: 90.7%). $^1\text{H NMR}$ (200

MHz, CDCl_3) δ : 1.39–1.52 (m, 18H), 1.70–1.90 (m, 4H), 1.91–2.02 (m, 2H), 2.45 (s, 3H), 2.60–2.70 (m, 1H), 3.95–4.15 (m, 2H), 4.16–4.25 (m, 1H), 5.10–5.19 (m, 1H), 7.37 (d, $J = 8.0$ Hz, 2H), 7.80 (d, $J = 8.2$ Hz, 2H). HRMS was calcd for $\text{C}_{25}\text{H}_{39}\text{N}_3\text{O}_7\text{S}$ ($\text{M} + \text{NH}_4$) $^+$: 514.2587. Found: 514.2589.

Compound **13b** was prepared from **12b** (102 mg, 0.3 mmol), Et_3N (0.21 mL, 1.5 mmol), TsCl (115 mg, 0.6 mmol) and DMAP (4 mg, 0.03 mmol), following the same procedure described for compound **13a**. Compound **13b**: 100 mg (yield: 67.1%). $^1\text{H NMR}$ (200 MHz, CDCl_3) δ : 1.39–1.52 (m, 18H), 1.70–1.90 (m, 4H), 1.90–1.98 (m, 1H), 2.15–2.30 (m, 1H), 2.50 (s, 3H), 2.60–2.70 (m, 1H), 3.95–4.15 (m, 2H), 4.20–4.35 (m, 1H); 5.10–5.19 (m, 1H), 7.37 (d, $J = 8.2$ Hz, 2H), 7.80 (d, $J = 8.2$ Hz, 2H). HRMS was calcd for $\text{C}_{25}\text{H}_{39}\text{N}_3\text{O}_7\text{S}$ ($\text{M} + \text{NH}_4$) $^+$: 514.2587. Found: 514.2589.

(2S,4S)-tert-Butyl 2-(tert-Butoxycarbonylamino)-4-cyano-7-fluoroheptanoate (**14a**) and *(2S,4S)*-tert-Butyl 2-(tert-Butoxycarbonylamino)-4-cyano-7-fluoroheptanoate (**14b**). To a solution of tris(dimethylamino)sulfonium difluorotrimethylsilicate (TASF, 100 mg, 0.363 mmol) in 3 mL of DCM and 3 mL of DMF was added $\text{Et}_3\text{N}(\text{HF})_3$ (0.021 mL) dropwise followed by **13a** (35 mg, 0.072 mmol) in 3 mL of DCM. The mixture was then heated at 50°C overnight. The reaction was quenched by the addition of ice-cold water (5 mL) and diluted with 50 mL of EtOAc, and then washed with H_2O (15 mL \times 2) and brine (15 mL) and dried with MgSO_4 . The filtrate was evaporated in vacuo and the residue was purified by FC (EtOAc/hexanes = 2/8) to give 22 mg of colorless oil **14a** (yield: 88.8%). $^1\text{H NMR}$ (200 MHz, CDCl_3) δ : 1.39–1.52 (m, 18H), 1.70–1.90 (m, 4H), 1.91–2.10 (m, 2H), 2.12–2.26 (m, 1H), 2.66–2.80 (m, 1H), 4.20–4.32 (m, 1H), 4.51 (dt, $J = 46.4$ Hz, $J = 6.4$ Hz, 2H), 5.10–5.15 (m, 1H). HRMS was calcd for $\text{C}_{17}\text{H}_{33}\text{FN}_3\text{O}_4$ ($\text{M} + \text{NH}_4$) $^+$: 362.2455. Found: 362.2485.

Compound **14b** was prepared from **13b** (80 mg, 0.16 mmol), TASF (220 mg, 0.80 mmol), and $\text{Et}_3\text{N}(\text{HF})_3$ (0.046 mL) following the same procedure described for compound **14a**. Compound **14b**: 39 mg (yield: 70.8%). $^1\text{H NMR}$ (200 MHz, CDCl_3) δ : 1.39–1.52 (m, 18H), 1.70–1.92 (m, 4H), 1.91–2.30 (m, 2H), 2.70–2.85 (m, 1H), 4.20–4.35 (m, 1H), 4.51 (dt, $J = 48.2$ Hz, $J = 5.8$ Hz, 2H), 5.10–5.22 (m, 1H). HRMS was calcd for $\text{C}_{17}\text{H}_{33}\text{FN}_3\text{O}_4$ ($\text{M} + \text{NH}_4$) $^+$: 362.2455. Found: 362.2485.

(2S,4R)-2-Amino-4-carbamoyl-7-fluoroheptanoic Acid (**3**) and *(2S,4S)*-2-Amino-4-carbamoyl-7-fluoroheptanoic Acid (**4**). Compound **14a** (37 mg, 0.11 mmol) in concentrated HCl (1.2 mL) was stirred at rt for 6 h. The pH was then adjusted to 7–8 with 5% ammonium solution. The neutralized solution was submitted to a small column of Dowex 50WX8-200 (H^+ form, 10 g). The fraction containing product was concentrated in vacuo and dried under high vacuum overnight to afford the crude product as a white solid. It was further purified by recrystallization from EtOH/ H_2O to provide 5.9 mg of white solid **4** (yield: 26.0%). $^1\text{H NMR}$ (200 MHz, D_2O) δ : 1.49–1.56 (m, 3H), 1.57–1.80 (m, 1H), 1.80–1.95 (m, 2H), 2.51–2.59 (m, 1H), 3.45–3.52 (m, 1H), 4.51 (d.t, $J = 46.4$ Hz, $J = 6.4$ Hz, 2H); $^{13}\text{C NMR}$ (200 MHz, D_2O) δ : 179.8, 174.0, 84.82 (d, $J = 157.5$ Hz), 53.0, 42.2, 33.4, 27.2 (d, $J = 20$ Hz), 28.1. HRMS was calcd for $\text{C}_8\text{H}_{16}\text{FN}_2\text{O}_3$ ($\text{M} + \text{NH}_4$) $^+$: 207.1145. Found: 207.1169.

Compound **3** was prepared from **14b** (39 mg, 0.11 mmol) and concentrated HCl (1.2 mL) following the same procedure described for compound **4**. Compound **3**: 6.8 mg (yield: 30%). $^1\text{H NMR}$ (200 MHz, D_2O) δ : 1.49–1.70 (m, 4H), 1.70–1.90 (m, 1H), 2.01–2.15 (m, 1H), 2.40–2.50 (m, 1H), 3.42–3.56

(m, 1H), 4.41 (dt, $J = 47.4$ Hz, $J = 5.0$ Hz, 2H). ^{13}C NMR (50 MHz, D_2O) δ : 179.9, 174.0, 84.82 (d, $J = 157.5$ Hz), 53.0, 42.1, 33.4, 27.4 (d, $J = 30$ Hz). HRMS was calcd for $\text{C}_8\text{H}_{16}\text{FN}_2\text{O}_3$ ($\text{M} + \text{NH}_4$) $^+$: 207.1145. Found: 207.1162.

(S)-5-Benzyl 1-tert-Butyl 2-(tert-Butoxycarbonylamino)pentanedioate (16). To a solution of Boc-Glu(OBzl)-OH, **15**, (3.37 g, 10 mmol) in 20 mL of DCM was added *tert*-butyl 2,2,2-trichloroacetimidate (3.9 g, 18 mmol) in 20 mL of cyclohexane dropwise. The mixture was stirred at rt for 5 min. $\text{BF}_3 \cdot \text{Et}_2\text{O}$ (0.12 mL, 1 mmol) was added dropwise. The reaction mixture was stirred at rt for 4 h. The solid was filtered off. The filtrate was evaporated in vacuo and the residue was purified by FC (EtOAc/hexanes = 2/8) to give 3 g of white solid **16** (yield: 76.3%). ^1H NMR (200 MHz, CDCl_3) δ : 1.44–1.46 (m, 18H), 1.90–1.97 (m, 1H), 2.13–2.20 (m, 1H), 2.40–2.50 (m, 2H), 4.20–4.23 (m, 1H), 5.06 (s, 1H), 5.13 (s, 2H), 7.36 (s, 5H). HRMS was calcd for $\text{C}_{21}\text{H}_{32}\text{NO}_6$ ($\text{M} + \text{H}$) $^+$: 394.2230. Found: 394.2241.

(2S,4S)-1-Benzyl 5-tert-Butyl 2-Allyl-4-(tert-Butoxycarbonylamino)pentanedioate (17). LiHMDS solution (8.8 mL, 1 M in THF) was added to a three-necked 250 mL flask and cooled down to -78 °C. Compound **16** (1.57 g, 4 mmol) was dissolved in 6 mL of THF was then added dropwise over 30 min. The mixture was stirred at -78 °C for another 2 h. Allyl bromide (2.4 g, 20 mmol, 1.72 mL) was added dropwise. The mixture was then stirred at -78 °C for another 4 h. The reaction was quenched with 20 mL of ethyl acetate and 15 mL of HCl (2 M), the mixture was extracted with ethyl acetate (3 \times 25 mL). The organic layer was dried over MgSO_4 and filtered. The filtrate was concentrated, and the residue was purified by FC (EtOAc/hexane = 2/8) to give 1 g of colorless oil **17** (yield: 58%). ^1H NMR (200 MHz, CDCl_3) δ : 1.45–1.47 (m, 18H), 1.94–2.01 (m, 2H), 2.37–2.44 (m, 2H), 2.59–2.69 (m, 1H), 4.18–4.30 (m, 1H), 5.02–5.04 (m, 1H), 5.07–5.22 (m, 4H), 5.61–5.82 (m, 1H), 7.38 (s, 5H). HRMS was calcd for $\text{C}_{24}\text{H}_{36}\text{NO}_6$ ($\text{M} + \text{H}$) $^+$: 434.2543. Found: 434.2507.

(2S,4S)-1-Benzyl 5-tert-Butyl 4-(tert-Butoxycarbonylamino)-2-(3-hydroxypropyl)pentanedioate (18). To a solution of compound **17** (860 mg, 2 mmol) in 7 mL of THF was added 9-BBN (8 mL, 0.5 M solution in THF) dropwise at 0 °C. After stirring at 0 °C for 1 h, the reaction mixture was moved to rt and stirred for another 48 h. The mixture was then cooled in an ice-bath. H_2O_2 (2.2 mL of 30 wt % solution in H_2O) and NaOH (3 mL, 1 M) were added dropwise. The mixture was stirred at rt for 30 min, diluted with 15 mL H_2O , and extracted with ethyl acetate. The organic layer was dried over MgSO_4 and filtered. The filtrate was concentrated, and the residue was purified by FC (EtOAc/hexane = 1/1) to give 700 mg of colorless oil **18** (yield: 77.4%). ^1H NMR (200 MHz, CDCl_3) δ : 1.43–1.45 (m, 18H), 1.75–1.86 (m, 4H), 1.89–1.93 (m, 2H), 2.49–2.63 (m, 1H), 3.59 (t, $J = 6.4$ Hz, 2H), 4.24–4.27 (m, 1H), 5.04–5.1 (m, 3H), 7.36 (s, 5H). HRMS was calcd for $\text{C}_{24}\text{H}_{38}\text{NO}_7$ ($\text{M} + \text{H}$) $^+$: 452.2648. Found: 452.2623.

(2S,4S)-1-Benzyl 5-tert-Butyl 4-(tert-Butoxycarbonylamino)-2-(3-(tetrahydro-2H-pyran-2-yloxy)propyl)pentanedioate (19). To a solution of compound **18** (530 mg, 1.2 mmol) in 10 mL of DCM was added 3,4-dihydro-2H-pyran (225 μL , 2.4 mmol) and pyridinium *p*-toluenesulfonate (30 mg, 0.12 mmol). The mixture was stirred at rt for 3 h. The solvent was evaporated in vacuo and the residue was purified by FC (EtOAc/hexanes = 3/7) to give 578 mg of colorless oil **19** (yield: 90%). ^1H NMR (200 MHz, CDCl_3) δ : 1.43–1.45 (m, 18H), 1.50–1.64 (m, 6H), 1.68–1.73 (m, 4H), 1.90–2.01 (m,

2H), 2.53–2.60 (m, 1H), 3.30–3.53 (m, 2H), 3.64–3.87 (m, 2H), 4.11–4.21 (m, 1H), 4.53 (s, 1H), 4.89–4.93 (m, 1H), 5.15–5.31 (m, 2H), 7.36 (s, 5H). HRMS was calcd for $\text{C}_{29}\text{H}_{46}\text{NO}_8$ ($\text{M} + \text{H}$) $^+$: 536.3223. Found: 536.3201.

(2S,4S)-5-tert-Butoxy-4-(tert-butoxycarbonylamino)-5-oxo-2-(3-(tetrahydro-2H-pyran-2-yloxy)propyl)pentanoic acid (20). A mixture of the ester **19** (750 mg, 1.4 mmol) and 10% Pd/C (90 mg) in absolute EtOH (15 mL) was stirred under hydrogen overnight. This mixture was then filtered and the filtrate was concentrated to give 620 mg of colorless oil **20** (yield: 99%). ^1H NMR (200 MHz, CDCl_3) δ : 1.45–1.47 (m, 18H), 1.50–1.70 (m, 6H), 1.75–1.80 (m, 2H), 1.82–2.00 (m, 4H), 2.51–2.58 (m, 1H), 3.41–3.51 (m, 2H), 3.80–3.95 (m, 2H), 4.22–4.29 (m, 1H), 4.59 (s, 1H), 4.05–5.01 (m, 1H). HRMS was calcd for $\text{C}_{22}\text{H}_{40}\text{NO}_8$ ($\text{M} + \text{H}$) $^+$: 446.2754. Found: 446.2740.

(2S,4S)-tert-Butyl 2-(tert-Butoxycarbonylamino)-7-hydroxy-4-(2,4,6-trimethoxybenzylcarbonyl)heptanoate (21). To a solution of compound **20** (534 mg, 1.2 mmol) in 2 mL of DCM and 2 mL of DMF was added Et_3N (1.9 mmol, 0.26 mL), HOBt (1.44 mmol, 297 mg), 2,4,6-trimethoxybenzylamine hydrochloride (370 mg, 1.58 mmol), and *N,N*-dicyclohexylcarbodiimide (276 mg, 1.8 mmol) at 0 °C. The mixture was stirred at rt for 24 h. A total of 30 mL of EtOAc was added to the reaction mixture. The mixture was then washed with citric acid (10% in H_2O , 5 mL), H_2O (5 mL \times 2) as well as brine (5 mL), dried over Na_2SO_4 , and filtered. The filtrate was concentrated to give 624 mg of oil. The residue was dissolved in 4 mL of EtOH. Pyridinium *p*-toluenesulfonate (50 mg, 0.2 mmol) was then added. After heating at 50 °C for 4 h, the solvent was evaporated in vacuo and the residue was purified by FC (EtOAc/hexanes = 3/7) to give 203 mg of colorless oil **21** (yield: 30.8%). ^1H NMR (200 MHz, CDCl_3) δ : 1.44–1.45 (m, 18H), 1.46–1.70 (m, 4H), 1.81–1.86 (m, 2H), 2.14–2.21 (m, 2H), 3.54–3.60 (m, 2H), 3.82 (s, 9H), 4.12–4.18 (m, 1H), 4.28–4.37 (m, 1H), 4.53–4.62 (m, 1H), 5.04–5.09 (m, 1H), 5.95 (s, 1H), 6.13 (s, 1H). HRMS was calcd for $\text{C}_{27}\text{H}_{45}\text{N}_2\text{O}_9$ ($\text{M} + \text{H}$) $^+$: 541.3125. Found: 541.3083.

(2S,4S)-tert-Butyl 2-(tert-Butoxycarbonylamino)-7-(tosyloxy)-4-(2,4,6-trimethoxybenzylcarbonyl)heptanoate (22). To a solution of compound **21** (200 mg, 0.37 mmol) in 10 mL of DCM was added 4-(dimethylamino)pyridine (4.55 mg, 0.037 mmol), Et_3N (147 mg, 1.11 mmol), and TsCl (105 mg, 0.55 mmol) at 0 °C. The mixture was stirred at rt overnight. The reaction was then quenched with 15 mL of H_2O and extracted with ethyl acetate (15 mL \times 3). The organic layer was dried over MgSO_4 and filtered. The filtrate was concentrated, and the residue was purified by FC (EtOAc/hexane = 3/7) to give 209 mg of white solid **22** (yield: 81.7%). ^1H NMR (200 MHz, CDCl_3) δ : 1.44–1.45 (m, 18H), 1.55–1.62 (m, 4H), 1.76–1.89 (m, 2H), 1.93–2.07 (m, 1H), 2.47 (s, 3H), 3.82–3.84 (m, 9H), 3.94–4.04 (m, 2H), 4.04–4.10 (m, 1H), 4.28–4.37 (m, 1H), 4.56–4.66 (m, 1H), 4.95–4.99 (m, 1H), 5.89–5.94 (m, 1H), 6.14 (s, 1H), 7.35 (d, $J = 8.0$ Hz, 2H), 7.76 (d, $J = 8.4$ Hz, 2H). HRMS was calcd for $\text{C}_{34}\text{H}_{51}\text{N}_2\text{O}_{11}\text{S}$ ($\text{M} + \text{H}$) $^+$: 695.3214. Found: 695.3099.

(2S,4S)-1-Benzyl 5-tert-Butyl 4-(tert-Butoxycarbonylamino)-2-(3-(tosyloxy)propyl)pentanedioate (23). Compound **23** was prepared from **18** (0.370 g, 0.84 mmol), Et_3N (424 mg, 4.20 mmol), TsCl (319 mg, 1.68 mmol), and DMAP (10.2 mg, 0.084 mmol) in 10 mL of DCM, with the same procedure described for compound **22**. Compound **23**: 410 mg (yield: 80.5%). ^1H NMR (200 MHz, CDCl_3) δ : 1.42(s, 9H), 1.45(s,

9H), 1.48–1.60 (m, 4H), 1.77–1.95 (m, 2H), 2.45–2.51 (m, 4H), 3.97–3.99 (m, 2H), 4.08–4.18 (m, 1H), 4.90 (d, 1 H, $J = 9.2$ Hz), 5.10 (dd, 2H, $J = 12.2$ Hz, $J = 22$ Hz), 7.32–7.35 (m, 7H), 7.77 (d, 2H, $J = 8.2$ Hz). HRMS was calcd for $C_{31}H_{44}NO_3S$ ($M + H$)⁺: 606.2737. Found: 606.2784.

(2S,4S)-1-Benzyl 5-tert-Butyl 4-(tert-Butoxycarbonylamino)-2-(3-fluoropropyl)pentanedioate (24). To a solution of tris(dimethylamino)sulfonium difluorotrimethylsilicate (1.31 g, 4.75 mmol) in 5 mL of THF and 5 mL of DMF was added $Et_3N(HF)_3$ (0.273 mL) dropwise followed by **23** (0.700 g, 1.16 mmol) in 5 mL of THF. The mixture was then heated at 45 °C overnight. The reaction was quenched by the addition of ice-cold water (5 mL) and diluted with 100 mL of EtOAc, then washed with H_2O (25 mL \times 2) and brine (25 mL), and dried with $MgSO_4$. The filtrate was evaporated in vacuo and the residue was purified by FC (EtOAc/hexanes = 2/8) to give 0.430 g of colorless oil **24** (yield: 82.0%). ¹HNMR (200 MHz, $CDCl_3$) δ : 1.43 (s, 9H), 1.45 (s, 9H), 1.59–1.72 (m, 4H), 1.92–2.00 (m, 2H), 2.51–2.61 (m, 1H), 4.15–4.30 (m, 2H), 4.51–4.53 (m, 1H), 4.93 (d, 1H, $J = 8.4$ Hz), 5.13 (dd, 2H, $J = 12.2$ Hz, $J = 23$ Hz), 7.31–7.36 (m, 5H). HRMS was calcd for $C_{24}H_{37}FNO_6$ ($M + H$)⁺: 454.2605. Found: 454.2667.

(2S,4S)-5-tert-Butoxy-4-(tert-butoxycarbonylamino)-2-(3-fluoropropyl)-5-oxopentanoic acid (25). A mixture of the ester **24** (0.430 g, 0.95 mmol) and 10% Pd/C (0.100 g) in absolute EtOH (10 mL) was stirred under hydrogen overnight. This mixture was then filtered, and the filtrate was concentrated under vacuum to give 0.345 g of colorless oil **25** (yield: 100%). ¹HNMR (200 MHz, $CDCl_3$) δ : 1.45 (s, 9H), 1.47 (s, 9H), 1.61–1.83 (m, 4H), 1.91–2.03 (m, 2H), 2.43–2.62 (m, 1H), 4.17–4.39 (m, 2H), 4.51–4.67 (m, 1H), 5.06 (d, 1H, $J = 9.2$ Hz). HRMS was calcd for $C_{17}H_{31}FNO_6$ ($M + H$)⁺: 364.2135. Found: 364.2166.

(2S,4S)-tert-Butyl 2-(tert-Butoxycarbonylamino)-7-fluoro-4-(2,4,6-trimethoxybenzylcarbonyl)heptanoate (26). To a solution of **25** (0.345 g, 0.95 mmol), *N*-(3-(dimethylamino)propyl)-*N*-ethylcarbodiimide hydrochloride (0.258 g, 1.34 mmol) and 1-hydroxybenzotriazole hydrate (0.227 g, 1.34 mmol) was added triethylamine (0.485 g, 4.80 mmol) and 2,4,6-trimethoxybenzylamine hydrochloride (0.339 g, 1.45 mmol) at 0 °C. The solution was allowed to warm to rt. After stirred overnight, the mixture was diluted with 150 mL to EtOAc and washed with H_2O (30 mL \times 2) and brine (30 mL). The organic layer was dried by $MgSO_4$ and concentrated to give an oil that was purified by FC (EtOAc/hexane = 1/1) to give 0.350 g of colorless oil **26** (yield: 64.5%). ¹HNMR (200 MHz, $CDCl_3$) δ : 1.42 (s, 9H), 1.45 (s, 9H), 1.60–1.74 (m, 4H), 1.88–1.98 (m, 2H), 2.29–2.48 (m, 1H), 3.82 (s, 6H), 4.02–4.14 (m, 1H), 4.25–4.40 (m, 2H), 4.49–4.68 (m, 2H), 5.02 (br s, 1H), 6.20 (s, 2H), 6.34 (br s, 1H). HRMS was calcd for $C_{27}H_{44}FN_2O_8$ ($M + H$)⁺: 543.3082. Found: 543.3048.

Radiolabeling. [¹⁸F]Fluoride was purchased from IBA Molecular (Somerset, NJ) as an [¹⁸O]enriched aqueous solution of [¹⁸F]fluoride. Solid-phase extraction (SPE) cartridges such as Sep-Pak QMA Light and Oasis HLB cartridges were purchased from Waters (Milford, MA). High-performance liquid chromatography (HPLC) was performed on Agilent 1100 or 1200 series system with different HPLC columns.

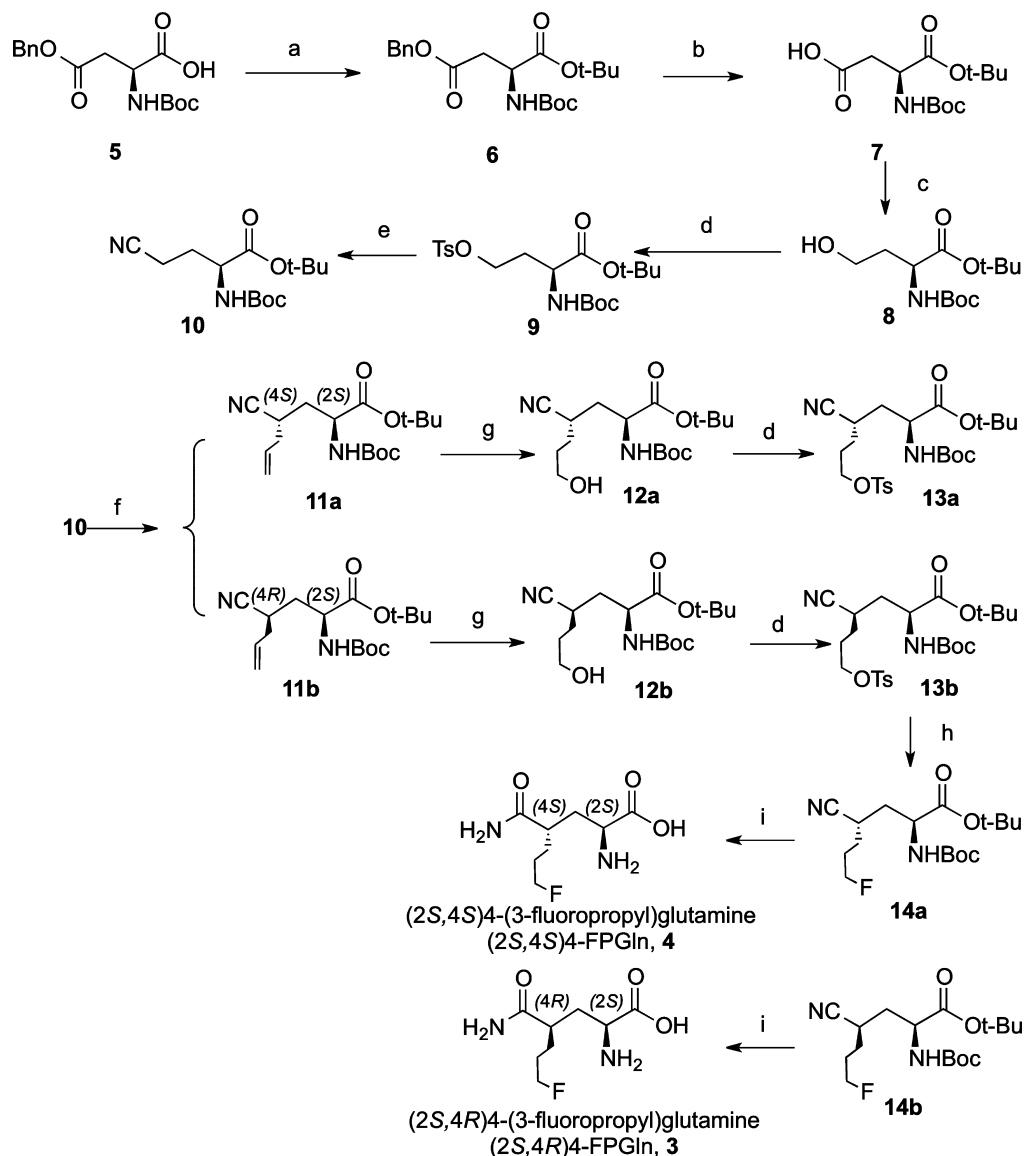
[³H]Gln was purchased from PerkinElmer (Waltham, MA) with >97% radiochemical purity and 1.11–2.22 TBq/mmol specific activity.

The radiosynthesis was performed by a similar method as described previously.⁹ Briefly, an activated SepPak Light QMA Carb was loaded with [¹⁸F]fluoride (740 to 1480 MBq (20 to 40 mCi)) and eluted with 1 mL of 18-crown-6/ $KHCO_3$ (160 mg of 18-crown-6 in 18.6 mL of ACN/29 mg of $KHCO_3$ in 3.4 mL of water). The solution was blown with argon until dry and dried twice azeotropically with 1 mL of acetonitrile at 80 °C under a flow of argon. The dried [¹⁸F]fluoride was cooled in an ice bath and 5 mg of tosylate precursor (O-tosylate, **13a** and **13b**, respectively) was dissolved in 0.5 mL of DMSO and added to the dried [¹⁸F]fluoride. The mixture was heated for 10 min at 110 °C in an oil bath. The mixture was then cooled in an ice bath and added to 6 mL of water/1 mL of acetonitrile. The mixture was loaded onto an activated Oasis HLB 3 cm³ cartridge, pushed through, and washed twice with 3 mL of water. The desired radiolabeled compound was eluted with 1 mL of acetonitrile. The acetonitrile solution was blown until dry. A mixture of 400 μ L of TFA/100 of μ L concentrated H_2SO_4 was added and heated for 10 min at 120 °C in a capped 10 mL vial. TFA was removed under argon while still warm. The reaction tube was then cooled in an ice bath. Water (1 mL) was slowly added and the mixture was neutralized by the slow addition of a saturated Na_2CO_3 solution under heavy shaking (\sim 1000 μ L) (pH \sim 8). The mixture was put through an activated Oasis HLB 3 cm³, which was topped with \sim 0.3 g of Ag11-A8 resin. The radioactivity was eluted with phosphate buffered saline (pH 7.0) in fractions of 0.5 mL volume to yield the desired radioactive [¹⁸F](2S,4R)-4-FPGln, **3**, and [¹⁸F](2S,4S)-4-FPGln, **4**, respectively.

The radiochemical and stereochemical purities were determined by two different HPLC systems. **System 1.** Column: Gemini 3u C18 150 \times 4.6 mm, 3 μ m. Mobile phase (gradient) Solvent A: ACN. Solvent B: 0.1% FA. Gradient, 1 mL/min: 0–3 min 95% B, 3–11 min 95%–5% B, 11–19 min 5%–95% B, 19–21 min 95% B. Retention times for both **3** and **4** are \sim 2.5 min. **System 2.** Column: Chirex 3126 (D)-penicillamine 250 \times 4.6 mm, 4.6 μ m. Mobile phase (isocratic): 2 mM $CuSO_4$ solution, 1 mL/min, column temperature at 30 °C. The retention times of **3** and **4** are 14.6 and 20 min, respectively.

Alternatively, TmobNH precursor, **22**, was used under a similar labeling condition as described above (18-crown-6/ $KHCO_3$ /ACN/80 °C/20 min). It was found that the TmobNH intermediate, **26**, was formed with a lower yield of $6.6 \pm 1.6\%$, radiochemical purity 98% ($n = 3$). The ¹⁸F intermediate, [¹⁸F]**26**, displayed the same profile on the HPLC as that of the “cold” compound. Deprotection was performed with 500 μ L of TFA at 40 °C for 8 min. Volatiles were removed under argon while still warm. The residue was treated with 1 mL of phosphate buffered saline (PBS) and filtered through a 0.45 μ filter and washed with 0.1 mL of PBS (pH 7.0) to give a crude dose. The solution was passed through an activated cartridge (Oasis HLB 3 cm³). The solid-phase extraction was further rinsed with 0.3 mL of PBS (pH 7.0) to yield (2S,4S)[¹⁸F]4-FPGln, **4**.

Cell Uptake Studies. 9L cells (ATCC, Manassas, VA) were cultured in Dulbecco's Modified Eagle's Medium (DMEM, GIBCO BRL, Grand Island, NY) supplemented with 10% fetal bovine serum (Hyclone, Logan, UT) and 1% 100 units/mL penicillin, 100 μ g/mL streptomycin. The cells were maintained in T-75 culture flasks under humidified incubator conditions (37 °C, 5% CO_2) and were routinely passaged at confluence.

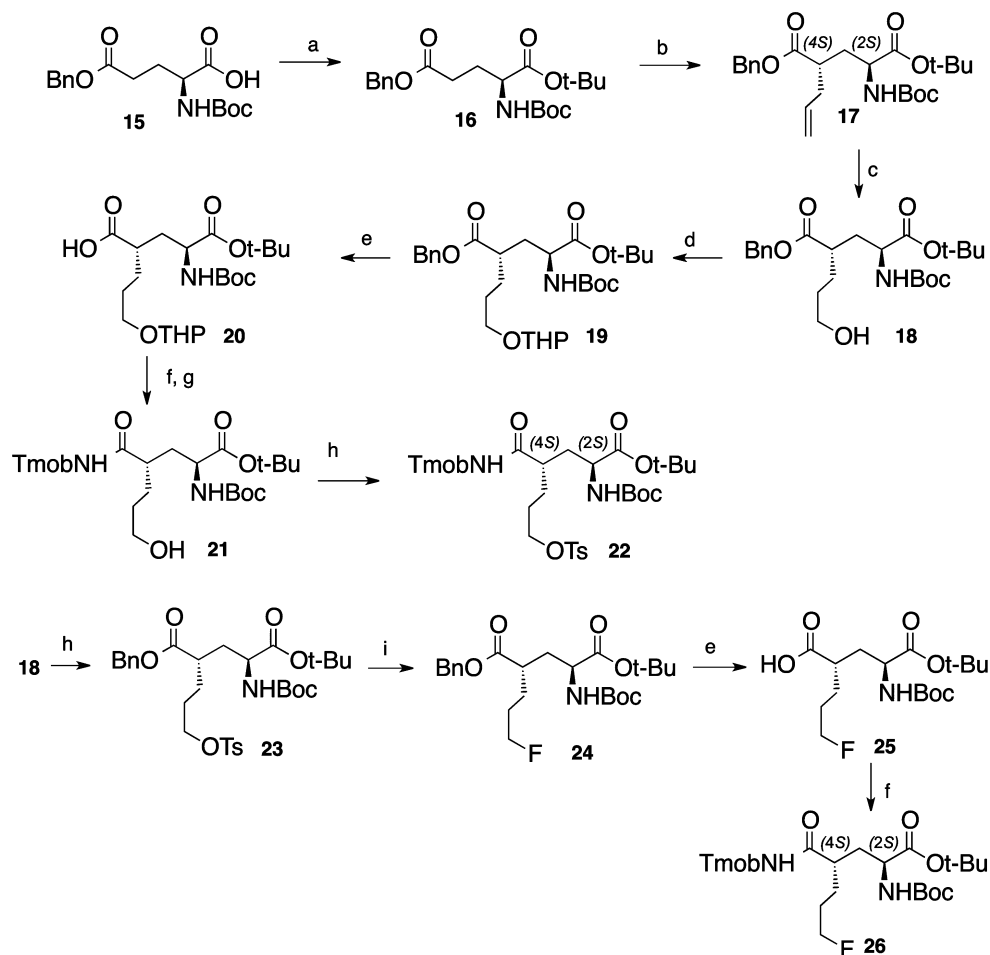
Scheme 1. Production of [^{18}F](2*S*,4*R*)-4-(3-fluoropropyl)glutamine^a

^aReagents and reaction conditions: (a) *tert*-butyl 2,2,2-trichloroacetimidate (TBTA), $\text{BF}_3 \cdot \text{Et}_2\text{O}$, DCM, cyclohexane, rt, overnight; (b) Pd/C, H_2 , MeOH, rt, overnight; (c) ECF, NaBH_4 , THF, H_2O , -15 – 0 °C, 4 h; (d) TsCl, Et_3N , DMAP, DCM, rt, overnight; (e) NaI, KCN, DMF, overnight; (f) LiHMDS, Allyl bromide, THF, -78 °C, 4 h; (g) 9-BBN, H_2O_2 , NaOH, 0 °C - rt, 48 h; (h) TASF, $\text{Et}_3\text{N}(\text{HF})_3$, DCM, DMF, 50 °C, overnight; (i) HCl, rt, 6 h.

Tumor cells were plated in 12 well plates 24 h prior to studies. On the day of the experiment, the culture media was aspirated and the cells were washed three times with warm PBS (containing 0.90 mM of Ca^{2+} and 1.05 mM of Mg^{2+}). [^{18}F](2*S*,4*R*)-4-FPGln, **3** (370 kBq) and L-[3,4- ^3H (N)]-glutamine ([^3H]Gln) (37 kBq) were mixed in PBS (with Ca^{2+} and Mg^{2+}) solution and then added to each well. The same procedure was performed with [^{18}F](2*S*,4*S*)-4-FPGln, **4** and [^3H]Gln. The cells were incubated at 37 °C for 5, 30, 60, and 120 min. At the end of the incubation period, the PBS solution containing the ligands was aspirated and the cells were washed three times with 1 mL of ice cold PBS (without Ca^{2+} and Mg^{2+}). After washing with ice-cold PBS, 350 μL of 0.1 N NaOH was used to lyse the cells. The lysed cells were collected onto filter paper and counted together with samples of the incubation dose using a gamma counter (Packard Cobra). After 24 h, ^3H activity was counted using a scintillation counter

(Beckman LS 6500). A total of 100 μL of the cell lysate was used to determine the protein concentration (Modified Lowry Protein Assay). The data was normalized as percentage uptake of initial dose (ID) relative to 100 μg of protein content (% ID/ 100 μg of protein).

Protein Incorporation of [^{18}F](2*S*,4*S*)-4-FPGln, **4, into 9L Tumor Cells.** To test the in vivo cell incorporation, we used 9L cells. Cells were plated (5×10^5 cells/well) on six-well plates in culture media 24 h prior to the experiment. On the day of experiment, the media was aspirated and the cells were washed three times with 4 mL of warm PBS (containing 0.90 mM of Ca^{2+} and 1.05 mM of Mg^{2+}). To measure the extent of protein incorporation of [^{18}F](2*S*,4*S*)-4-FPGln, **4**, protein bound activity in 9L cells was determined at 30 and 120 min after incubation. [^{18}F](2*S*,4*S*)-4-FPGln, **4** (370 kBq) and L-[3,4- ^3H (N)]-glutamine ([^3H]Gln, 37 kBq) in 2 mL of PBS were mixed in the incubation media.

Scheme 2. Production of [^{18}F](2*S*,4*S*)-4-(3-fluoropropyl)glutamine^a

^aReagents and conditions: (a) *tert*-butyl 2,2,2-trichloroacetimidate (TBTA), $\text{BF}_3 \cdot \text{Et}_2\text{O}$, DCM, cyclohexane, rt, overnight; (b) LiHMDS, Allyl bromide, THF, -78°C , 4 h; (c) 9-BBN, H_2O_2 , NaOH, 0°C –rt, 48 h; (d) DHP, PPTS, DCM, rt, 3 h; (e) Pd/C, H_2 , EtOH, rt, 6 h; (f) TmobNH₂·HCl, EDCI·HCl, HOBT, Et₃N, DCM, DMF, rt, 24 h; (g) PPTS, EtOH, 50°C , 4 h; (h) TsCl, Et₃N, DMAP, DCM, rt, overnight; (i) TASF, Et₃N(HF)₃, DCM, DMF, 50°C , overnight.

To identify the ligand's stability in supernatant after precipitation with trichloroacetic acid (TCA), cells were grown in 10 cm dishes and incubated with 1.8 MBq [^{18}F](2*S*,4*S*)-4-FPGln, **4**, only. At the end of incubation, the radioactive medium was removed, the cells were washed three times with ice cold PBS without Ca^{2+} and Mg^{2+} , treated with 0.25% trypsin, and resuspended in PBS. The samples were centrifuged (18 000g, 3 min), the supernatant removed, and the cells were suspended in 200 μL and 1% Triton-X 100 (Sigma, St. Louis, MO). After vortexing, 800 μL of ice cold 15% TCA was added to the solution. After precipitating for 10 min, the cells were centrifuged again (18 000g, 3 min) and washed twice with 15% ice cold TCA. The radioactivity of both gamma- and beta-emitting isotopes was determined separately for the supernatant and pellet. Protein incorporation was calculated as a percentage of acid precipitable activity.

In Vitro Transport Characterization Studies (Inhibition Studies). To characterize the transport of [^{18}F](2*S*,4*S*)-4-FPGln, **4**, competitive inhibition studies were conducted using the 9L cell line. The tracer was incubated at 37°C for 30 min. The cells were processed as described above. Various inhibitors were then added to the cells in concentrations ranging from 0.1 to 5 mM in PBS solution. Selected inhibitors included synthetic amino acid transport inhibitors such as *N*-

methyl- α -aminoisobutyric acid (MeAIB) for system A, and 2-amino-bicyclo[2.2.1] heptane-2-carboxylic acid (BCH) for system L.^{11–13} Natural amino acids, such as *L*-serine and *L*-glutamine, were also used as inhibitors, although they are not specific for a particular amino acid transport system. The data was compared in reference to uptake of [^{18}F](2*S*,4*S*)-4-FPGln, **4**, without any inhibitor in PBS solution at pH 7.4.

Biodistribution Studies in Rats Bearing 9L Tumors.

Studies of the *in vivo* distribution of [^{18}F](2*S*,4*S*)-4-FPGln, **4**, were performed in Fischer (F344) rats bearing 9L tumors as reported previously.⁸ F344 rats were purchased from Charles River Laboratories (Malvern, PA). 9L tumor cells ($\sim 10^6$) in PBS (0.2 mL) were injected subcutaneously into the lower right flank of the rat. The tumors took 12–15 days to reach appropriate size (1 cm diameter). All animals were fasted for 12–18 h prior to the study. Six rats per group were used for the biodistribution study. The rats were anesthetized with isoflurane (2–3%) and 0.2 mL of saline solution containing 25 μCi of the ligand was injected intravenously. The rats were sacrificed at 30 and 60 min postinjection by cardiac excision while under isoflurane anesthesia. The organs of interest were removed, weighed, and the radioactivity was counted with a gamma counter (Packard Cobra). The percent dose per gram

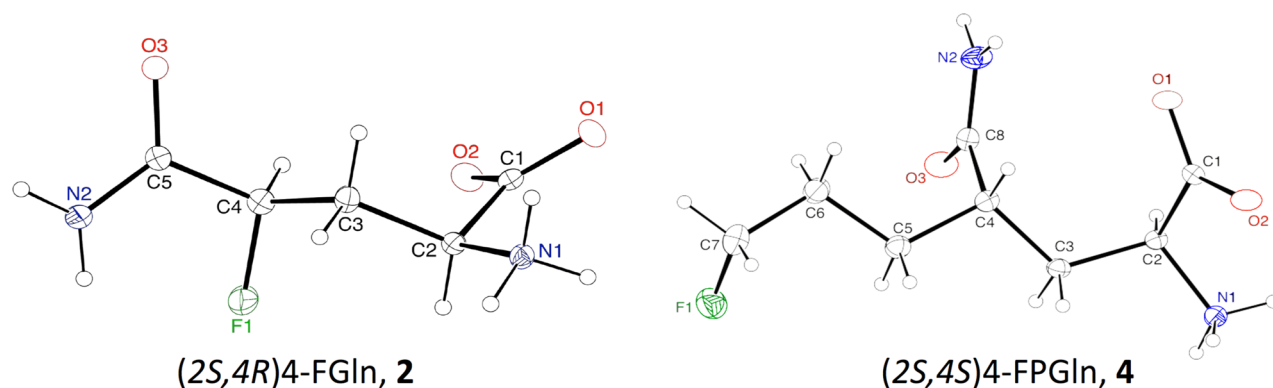


Figure 2. Comparison of X-ray crystallography structures for (2*S*,4*R*)-4-fluoro-glutamine, (2*S*,4*R*)-4-FGln, **2**,⁹ and (2*S*,4*S*)-4-(3-fluoropropyl)-glutamine, (2*S*,4*S*)-4-FPGln, **4**. ORTEP drawing of the title compounds were shown with 30% probability thermal ellipsoids. (Crystal structure, (2*S*,4*S*)-4-FPGln, **4**, was submitted to the Cambridge Crystallographic Data Centre (CCDC 991692).

was calculated by a comparison of the tissue activity counts to counts of 1% of the initial dose.

Small Animal Imaging Studies. Dynamic small animal PET (APET) imaging studies were conducted with [¹⁸F]-(2*S*,4*R*)-4-FGln, **2**, and [¹⁸F](2*S*,4*S*)-4-FPGln, **4** similar to that reported previously.⁸ All scans were performed on a dedicated animal PET scanner (Mosaic by Phillips) that has a field of view of 11.5 cm. F344 rats with 9L tumors were used for the imaging studies. A total of 22–37 MBq of activity was injected intravenously via the lateral tail vein. All animals were sedated with isoflurane anesthesia (2–3%, 1 L/min oxygen) and were then placed on a heating pad in order to maintain body temperature throughout the procedure. The animals were visually monitored for breathing and any other signs of distress throughout the entire imaging period. The data acquisition began after an intravenous injection of the tracer. All scans were conducted over a period of 120 min (dynamic, 5 min/frame). The frames were reconstructed and then analyzed with AMIDE imaging analysis software.

RESULTS

Synthesis. In order to produce [¹⁸F](2*S*,4*R*)-4-(3-fluoropropyl)glutamine, **3**, ([¹⁸F](2*S*,4*R*)-4-FPGln) and [¹⁸F]-(2*S*,4*S*)-4-(3-fluoropropyl)glutamine, **4** ([¹⁸F](2*S*,4*S*)-4-FPGln), we employed two different schemes (Schemes 1 and 2) for preparation of nonradioactive “cold” compounds (**3** and **4**) and the cyanide and -OTs precursors for radiolabeling. One approach was to prepare the corresponding protected 4-cyanide derivatives, which led to the formation of the desired final products. Commercially purchased Boc-Asp(OBzl)-OH, **5**, was treated with *tert*-butyl 2,2,2-trichloroacetimidate/BF₃·Et₂O at room temperature to give the *t*-BuO- ester, **6**; the BnO- ester group was converted to the acid, **7**, by Pd/C catalyzed hydrogenation. The aspartic acid, **7**, was carefully reduced with NaBH₄ in THF/water at –15 to 0 °C to the corresponding alcohol, **8**. The alcohol group was successfully converted to the cyanide, **10**, through the -OTs intermediate, **9**. The cyanide derivative, **10**, was treated with LiHMDS and allyl bromide at –78 °C to give (2*S*,4*S*)-*tert*-butyl 2-(*tert*-butoxycarbonylamino)-4-cyanohept-6-enoate (**11a**) and (2*S*,4*R*)-*tert*-butyl 2-(*tert*-butoxycarbonylamino)-4-cyanohept-6-enoate (**11b**) (**11a** to **11b** ratio of 2:1 in 28% and 15% isolated yields). A similar reaction was reported previously for preparation of allyl derivatives of aspartate using the dianionic allylation reactions of amino acid derivatives.¹⁴ The allyl derivatives, **11a** and **11b**,

were separated and purified by flash chromatography. They were converted to the corresponding alcohols, **12a** and **12b**, and following the treatment with tosyl chloride to the O-tosylated **13a** and **13b** in good yields. The O-tosylated **13a** and **13b** were treated with TASF, Et₃N(HF)₃, DCM, DMF, 50 °C, overnight to give the desired **14a** and **14b**, in good yields. Optimization of the fluorination reaction condition using TASF and Et₃N(HF)₃, as the reagents was reported previously for the preparation of 4-fluoroglutamine.⁹ Deprotection using hydrochloric acid at room temperature produced the final end products, [¹⁸F](2*S*,4*R*)-4-(3-fluoropropyl)glutamine, **3**, and [¹⁸F](2*S*,4*S*)-4-(3-fluoropropyl)glutamine, **4**. The O-tosylated **13a** and **13b** were also successfully used for the radiolabeling reaction (see Discussion below).

The second method introduced N-Tmob protected precursors (as a protecting group to preserve the amide) for radiolabeling and deprotection. Previously, we have tested for the preparation of N-Tmob protected precursors for making isomers of 4-fluoroglutamine (4-FGln).⁹ We successfully developed ¹⁸F labeling using this precursor under different labeling conditions. We wanted to extend the same method to the synthesis and labeling of [¹⁸F](2*S*,4*S*)-4-(3-fluoropropyl)-glutamine, **4**. To achieve this, we started with commercially available, Boc-Glu(OBzl)-OH, **15**. After treating with *tert*-butyl 2,2,2-trichloroacetimidate/BF₃·Et₂O at room temperature, it gave the *t*-Bu ester, **16**. Using the same dianionic allylation reactions of amino acid derivatives,¹⁴ the reaction preferentially produced the protected (2*S*,4*S*)-4-allyl-glutamate (in 58% yield). It is interesting to note that the reaction led to the (2*S*,4*S*) isomer only. The allyl group was converted to alcohol, **18**, by 9-BBN/H₂O₂/NaOH in 0 °C. The alcohol was protected by THP, and the O-benzyl ester was hydrolyzed and the acid, **20**, was transformed to Tmob-protected amide, **21**. The alcohol, **21**, was treated with tosyl chloride to the O-tosylated, **22**, which is a suitable precursor for a radioactive ¹⁸F labeling reaction. In order to provide an authentic sample, a cold standard, for the first step of the radioactive ¹⁸F labeling reaction, we also prepared compound, **26**.

To further confirm the chemical structure, a slow evaporating recrystallization method provided excellent crystals of “cold” (2*S*,4*S*)-4-FPGln, **4** and the X-ray crystallographic analysis data added support to the structure assignment (Figure 2). The optically pure (2*S*,4*S*)-4-FPGln, **4**, has never been prepared and presented before. In the X-ray crystallographic structures of (2*S*,4*R*)-4-FGln, **2**, and (2*S*,4*S*)-4-FPGln, **4**, the amino acid

Additional studies may be needed to investigate the optical preferences in the substitution of O-Ts with [^{18}F]fluoride. To improve the radiolabeling reaction for the more promising [^{18}F](2*S*,4*S*)-4-FPGln, **4**, we made the effort to use a different O-tosylated TmobNH-protected precursor, **22**. A similar 4-O-tosylated TmobNH-protected precursor was successfully employed for substitution of O-Ts with [^{18}F]fluoride using similar reaction conditions to give the desired [^{18}F](2*S*,4*R*)-4-FGln, **2**, in good radiochemical yields (30–40%).⁹ However, much to our surprise, the radiochemical yield for precursor, **22**, gave a lower labeling yield. The decay corrected radiochemical yield was $2.7 \pm 0.9\%$, $n = 3$.

In Vitro Cell Uptake and Inhibition Study in 9L Tumor Cells. In order to test the specificity of this radiotracer, in vitro cell uptake and inhibition studies were performed in 9L cells. Both [^{18}F](2*S*,4*R*)-4-FPGln, **3**, and [^{18}F](2*S*,4*S*)-4-FPGln, **4**, displayed excellent uptake in the 9L tumor cells in vitro. At all time points studied (5 to 120 min), both tracers displayed very similar values (Figure 4). It appeared that the stereoisomers 4*S*

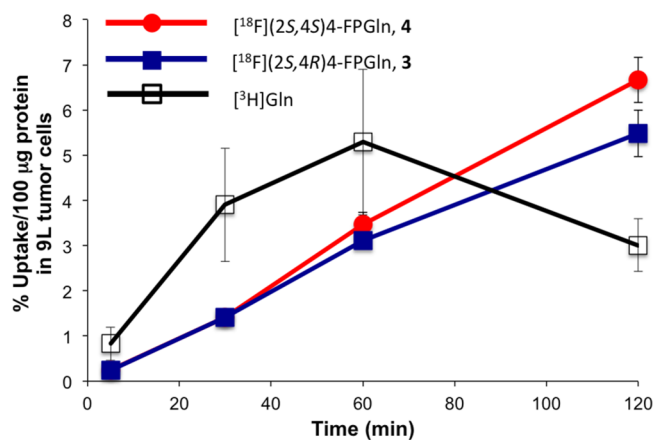


Figure 4. In vitro cell uptakes of [^{18}F](2*S*,4*R*)-4-FPGln, **3**, and [^{18}F](2*S*,4*S*)-4-FPGln, **4**. [^3H]Gln was used as a standard. All radiotracers were evaluated in the 9L tumor cell line.

and 4*R* have comparable tumor cell uptakes. Because of this observation, we only used the [^{18}F](2*S*,4*S*)-4-FPGln, **4**, tracer in further investigations on inhibition of cell uptakes and for the in vivo biological studies. The tracer, [^{18}F](2*S*,4*S*)-4-FPGln, **4**, was incubated at 37 °C for 30 min with different amino acid transport inhibitors. The results in Figure 5 suggested that the system A inhibitor, MeAIB (*N*-methyl- α -aminoisobutyric acid), had no inhibitory effect on the uptake, indicating that the system A amino acid transport was not involved in the uptake of this new tracer. System L inhibitor, BCH (2-aminobicyclo[2.2.1] heptane-2-carboxylic acid), System ASC inhibitor L-serine (L-Ser) and System ASC (SLC1A5), N inhibitor, L-glutamine (L-Gln), exhibited similar concentration dependent reduction of cell uptake, thus indicating potential involvement of system L, ASC, and N in the uptake (Figure 5).

Protein Incorporation of [^{18}F](2*S*,4*S*)-4-FPGln, **4, into 9L Tumor Cells.** One of the important issues to consider when developing tracers to image glutamine metabolism in tumors is the protein incorporation of the tracer once inside the cells. After incubation of [^{18}F](2*S*,4*S*)-4-FPGln, **4**, and [^3H]Gln with 9L tumor cells, the cell lysates were treated with TCA and the radioactivity in the precipitates and supernatant were counted. Results showed that the majority of [^3H]Gln activity was associated with the TCA precipitates suggesting that most of

the [^3H]Gln (>90%) was incorporated into macromolecules, whereas the glutamine analog, [^{18}F](2*S*,4*S*)-4-FPGln, **4**, remained predominantly in the supernatant (no incorporation).

On the basis of the protein incorporation data above (Figure 6), [^{18}F](2*S*,4*S*)-4-FPGln, **4**, behaved very differently from that of [^3H]Gln. It is reasonable to conclude that the new probe, [^{18}F](2*S*,4*S*)-4-FPGln, **4**, is not associated with intracellular macromolecules, and thus, it is less likely to measure the intracellular metabolism associated with glutamine metabolism.

Biodistribution in F344 Rats Bearing 9L Tumor.

Biodistribution studies of [^{18}F](2*S*,4*S*)-4-FPGln, **4**, were conducted in F344 rats (125–149 g, $n = 4$) bearing 9L tumors on their thigh. This is a well-established animal model that resembles typical human glioblastomas in clinical settings.¹⁵ Rats were sacrificed at 30 and 60 min postinjection by cardiac excision while under isoflurane anesthesia. [^{18}F](2*S*,4*S*)-4-FPGln, **4**, showed respectable uptake within the 9L tumors, displaying 0.83% dose/g uptake at 30 min post injection. Tumor uptake and retention slowly washed out of the 9L tumor to 0.60% dose/g. At 30 min, tumor-to-background (tumor-to-muscle, tumor-to-blood, and tumor-to-brain) ratios of [^{18}F](2*S*,4*S*)-4-FPGln, **4**, were 6.91, 1.45, and 5.53, respectively. The highest uptake of [^{18}F](2*S*,4*S*)-4-FPGln, **4**, was found in the pancreas. High pancreatic uptake is consistent with the fact that amino acids are precursors for digestive enzymes actively produced in the pancreas. Low bone (femur) uptake was observed at 30 min (0.53% dose/g) and it stayed at that value at 60 min post injection.

Preliminary PET imaging studies of [^{18}F](2*S*,4*S*)-4-FPGln, **4**, in rats with 9L tumors showed that the probe was clearly taken up by the tumors ($n = 3$) (Figure 7). To further investigate the tumor uptake, dynamic small animal PET studies using one rat bearing two 9L tumors were carried out on two different days with either [^{18}F](2*S*,4*S*)-4-FPGln, **4**, or [^{18}F](2*S*,4*R*)-4-FGln, **2**. The direct comparison study using the same animal can avoid some of the complications related to differences in tumor growth in different animals. [^{18}F](2*S*,4*R*)-4-FGln, **2**, was recently reported as a tumor PET imaging agent for glutaminolysis.⁸ PET images of [^{18}F](2*S*,4*S*)-4-FPGln, **4**, and [^{18}F](2*S*,4*R*)-4-FGln, **2**, were selected for visualization (Figure 7). As these images demonstrate, the 9L tumors could be visualized with either of the ligands. High kidney, liver, and bladder uptake were also observed. Defluorination/bone uptake was more apparent in the images of [^{18}F](2*S*,4*R*)-4-FGln, **2**, compared to those of [^{18}F](2*S*,4*S*)-4-FPGln, **4**. To assess the in vivo kinetics, region-of-interest analysis was performed (using AMIDE software to generate the time-activity curves; Figures 8 and 9). The kinetic curves confirmed that all the tracers exhibited higher tumor uptake compared to the muscle (background) regions. [^{18}F](2*S*,4*S*)-4-FPGln, **4**, showed a higher tumor-to-muscle ratio than [^{18}F]4-FGln. Both ligands displayed similar kinetics. Both ligands had rapid tumor uptake and reached their maximum uptake within the first 20 min. Tumor uptake for [^{18}F]4-FGln remained rather consistent over 2 h, whereas [^{18}F](2*S*,4*S*)-4-FPGln, **4**, displayed a faster tumor washout rate. Also noteworthy, ([^{18}F](2*S*,4*S*)-4-FPGln, **4**, showed less defluorination/bone uptake in comparison to that of [^{18}F]4-FGln. Results of the in vivo PET imaging studies using the 9L tumor model suggested that the [^{18}F](2*S*,4*S*)-4-FPGln, **4**, localized in the 9L tumor as well, if not better, than [^{18}F](2*S*,4*R*)-4-FGln, **2**.

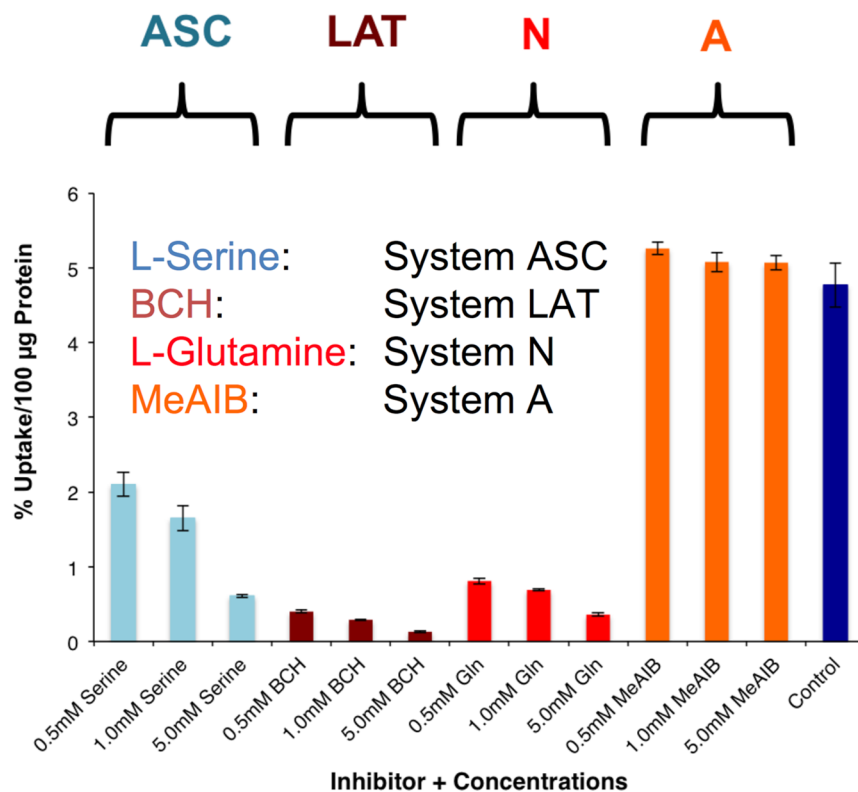


Figure 5. In vitro cell uptake inhibition studies of $[^{18}\text{F}](2\text{S},4\text{S})\text{-4-FPGln}$, **4**, conducted in 9L cells using inhibitors: System LAT inhibitor, BCH (2-amino-bicyclo[2.2.1] heptane-2-carboxylic acid); System ASC inhibitor, L-serine (L-ser), System A inhibitor, N-methyl- α -aminoisobutyric acid (MeAIB); and system N inhibitor, L-glutamine (L-Gln).

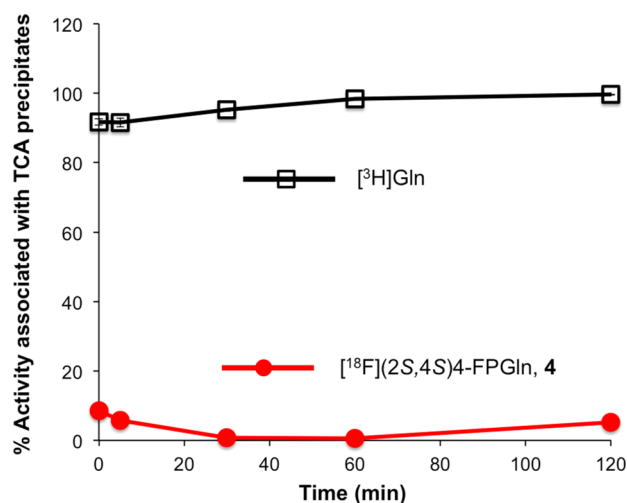


Figure 6. Incorporation of $[^{18}\text{F}](2\text{S},4\text{S})\text{-4-FPGln}$, **4**, and $[^3\text{H}]\text{Gln}$ into protein in 9L tumor cells was investigated. The comparison of cellular uptake of $[^{18}\text{F}](2\text{S},4\text{S})\text{-4-FPGln}$, **4**, and $[^3\text{H}]\text{Gln}$ was performed using dual-isotope experiments at 0, 5, 30, 60, and 120 min incubation time periods. Cell lysates were treated with TCA and the radioactivity (both ^{18}F and ^3H) associated with the TCA precipitates was counted.

DISCUSSION

Glutamine is found circulating in the blood as well as stored in skeletal muscles in high concentrations (0.5–1 mmol/L). Glutamine plays various critical functions: as an energy source and a substrate for DNA and protein synthesis, a primary source of fuel for cells lining the inside of the small intestine

Table 1. Tissue Distribution of Radioactivity^a in F344 Rats Bearing 9L Tumors after Intravenous Injection of $[^{18}\text{F}](2\text{S},4\text{S})\text{-4-FPGln}$, **4^b**

organ	30 min	60 min
blood	0.57 ± 0.02	0.38 ± 0.02
heart	0.31 ± 0.01	0.26 ± 0.02
muscle	0.12 ± 0.01	0.11 ± 0.01
lung	0.52 ± 0.01	0.39 ± 0.02
kidney	12.4 ± 1.02	8.93 ± 0.42
pancreas	3.22 ± 0.42	2.24 ± 0.06
spleen	0.59 ± 0.02	0.42 ± 0.03
liver	1.72 ± 0.07	1.58 ± 0.08
skin	0.47 ± 0.15	0.37 ± 0.06
brain	0.15 ± 0.00	0.16 ± 0.01
bone	0.53 ± 0.08	0.56 ± 0.17
9L tumor	0.83 ± 0.04	0.60 ± 0.06
tumor/blood	1.45 ± 0.08	1.57 ± 0.17
tumor/muscle	6.91 ± 0.66	5.45 ± 0.73

^aPercent dose/gram. ^bResults are expressed as mean ± SD (n = 4).

and rapidly dividing immune cells, and as a regulator of acid–base balance by producing ammonium in the kidneys. In the brain, the glutamine–glutamate shunt is a critical pathway to control the inhibitory and excitatory neuronal signals. Glutamine transporters play an important role in regulating mammalian cell functions. There are three known glutamine transporters, SLC1A5 (ASCT2, Km 20 mM), LAT1 (SLC7A5, Na⁺ independent), SNAT (Na⁺/neutral transporter).^{16–19} In the context of tumor growth, SLC1A5 is the most important glutamine transporter responsible for rapidly growing tumors. In these tumor cells, the expression of SLC1A5 is up-regulated.

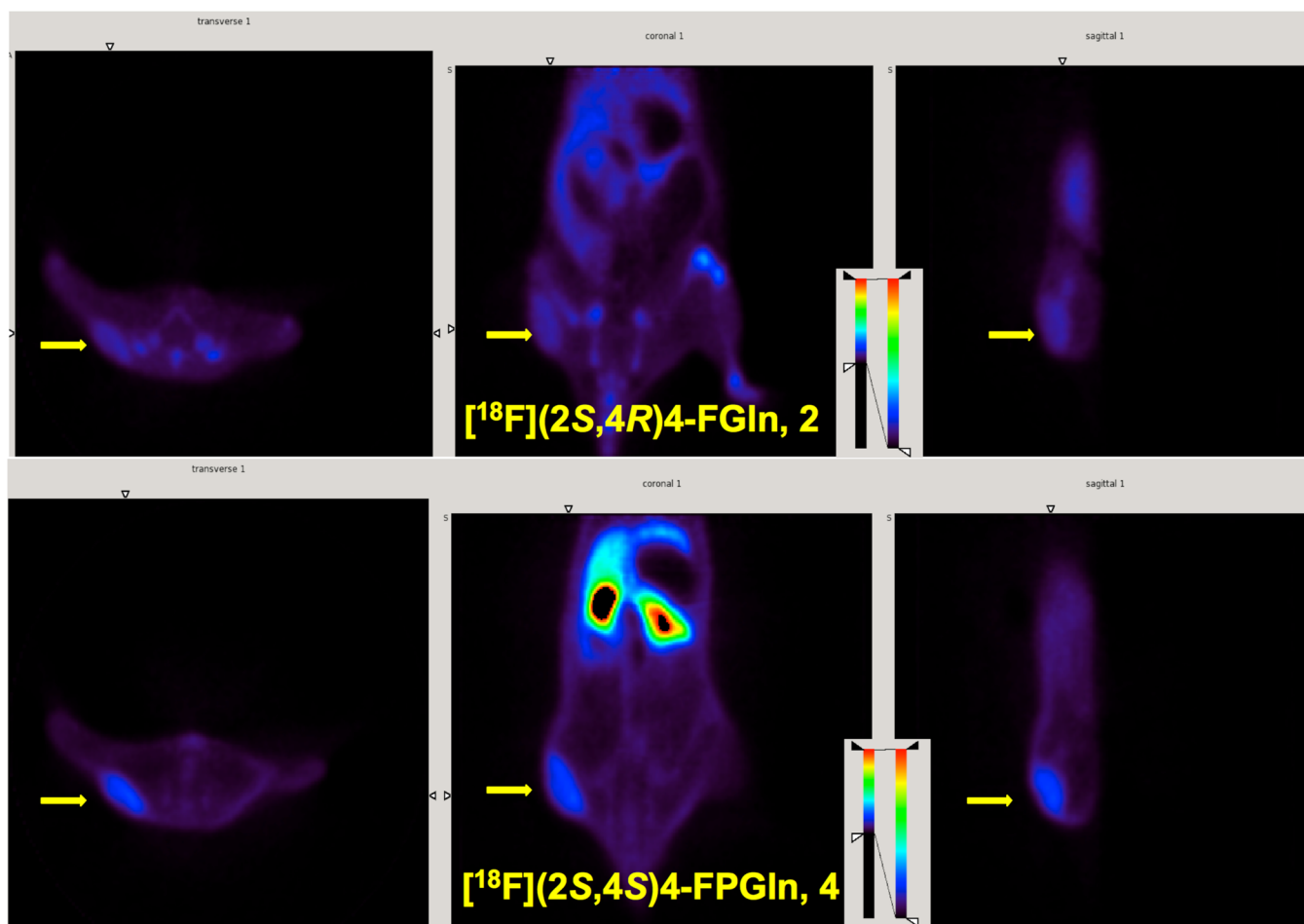


Figure 7. Representative PET images of 9L tumor bearing rats after intravenous injection of $[^{18}\text{F}](2\text{S},4\text{S})\text{-}4\text{-FPGln, 4}$, or $[^{18}\text{F}](2\text{S},4\text{R})\text{-}4\text{-FGln, 2}$ into a F344 rat bearing a 9L tumor. The images of the transverse, coronal, and sagittal views are from a summed 2 h scan. Arrows represent the location of tumors on the hind leg region of the F344 rat.

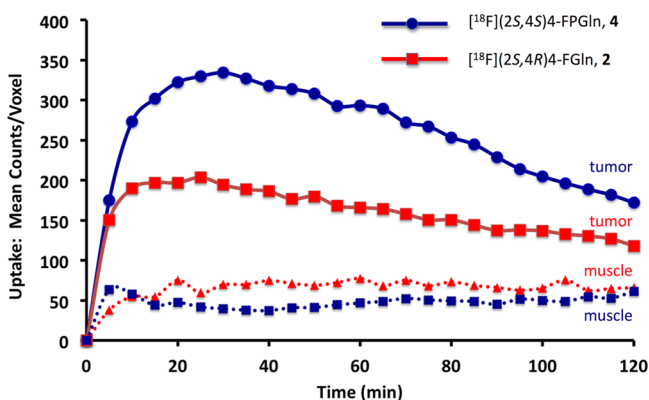


Figure 8. Time activity curves of tumor (target) and muscle (background) uptake in F344 rats bearing 9L tumors: (blue) $[^{18}\text{F}](2\text{S},4\text{S})\text{-}4\text{-FPGln, 4}$, and (red) $[^{18}\text{F}](2\text{S},4\text{R})\text{-}4\text{-FGln, 2}$.

Just as FDG-PET is useful for imaging tumors in which the glucose transporter is overexpressed, glutamine tracers will accumulate in these tumors. The tracer reported in this project appeared to be more sensitive to the inhibition by LAT inhibitor, BCH, not glutamine (SLC1A5). The relationship between amino acid transporter expression and tumor growth is a rapidly expanding research field. Many amino acid derivatives have been reported for imaging tumor growth based on

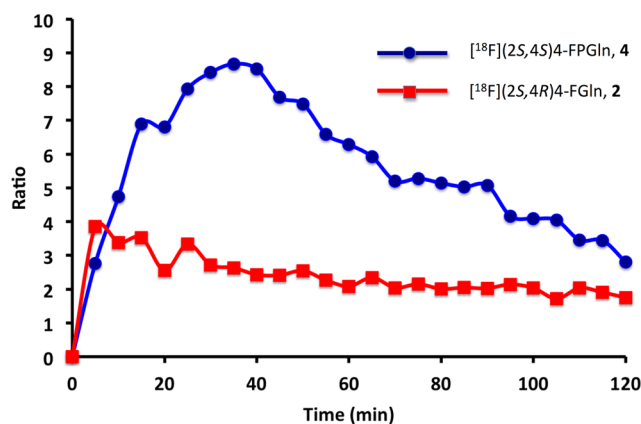


Figure 9. Comparison of ratios of tumor/muscle at different time points (0 to 120 min) for $[^{18}\text{F}](2\text{S},4\text{S})\text{-}4\text{-FPGln, 4}$, and $[^{18}\text{F}](2\text{S},4\text{R})\text{-}4\text{-FGln, 2}$.

different amino acid transporters,^{20,21} most of which were not designed to measure glutamine metabolism specifically. Recently, a detailed study of transport mechanisms of *trans*-1-amino-3-fluoro[1- ^{14}C]cyclobutanecarboxylic acid (anti-[^{14}C]-FACBC) has been published. The corresponding $[^{18}\text{F}]$ FACBC is now being tested in humans as a potential prostate tumor imaging agent.^{20,22–28} It may be desirable to

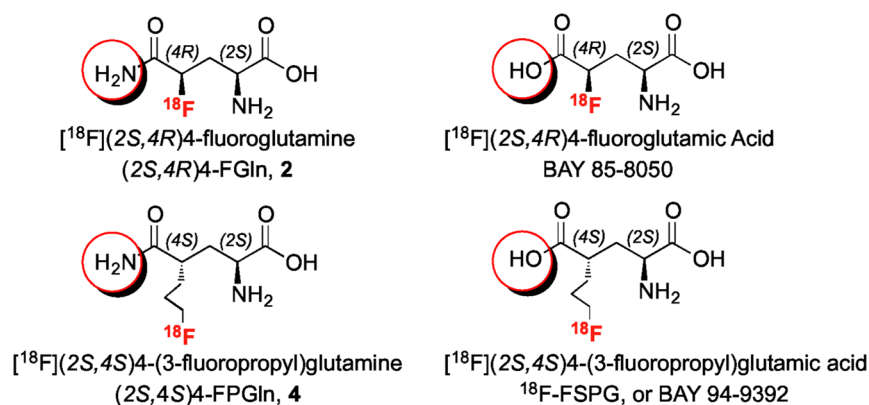


Figure 10. Chemical structures of analogs of glutamine and glutamic acid derivatives: $[^{18}\text{F}](2\text{S},4\text{R})$ -4-fluoroglutamine, $(2\text{S},4\text{R})$ -4-FGln, **2**, vs $[^{18}\text{F}](2\text{S},4\text{R})$ -4-fluoroglutamic Acid, BAY 85–8050; $[^{18}\text{F}](2\text{S},4\text{S})$ -4-(3-fluoropropyl)glutamine, $(2\text{S},4\text{S})$ -4-FPGln, **4**, vs $[^{18}\text{F}](2\text{S},4\text{S})$ -4-(3-fluoropropyl)glutamic acid, ^{18}F -FSPG, or BAY 94–9392. These two pairs of probes are structurally very similar, containing a C5 amide vs a C5 carboxylic acid group, but the mechanisms of uptake and retention are dramatically different.

further evaluate the significance of the observation on different levels of inhibition by LAT vs SLC1A5 subtypes of amino acid transporters.

$[^{18}\text{F}](2\text{S},4\text{R})$ -4-fluoroglutamic acid, BAY 85–8050 has been reported as a tumor imaging agent.²⁹ In order to improve the in vivo stability and to reduce defluorination in vivo, (4S) -4-(3- $[^{18}\text{F}]$ fluoropropyl)-L-glutamate (^{18}F -FSPG, or BAY 94–9392) was also prepared and tested.^{30–32} It was found that ^{18}F -FSPG, a glutamic acid containing a 3-fluoro-propyl substitution group at the C4 position, showed good tumor uptake and reduced in vivo defluorination.²⁹ In vivo human studies suggest that ^{18}F -FSPG is a tracer useful for assessing system xC^- (anionic amino acid) transporter activity in tumors with PET.^{31,32} Piramal Biotechnology is now developing the ^{18}F -FSPG for imaging tumors in which xC^- transporters are prominently expressed and oxidative stress is up-regulated.

The new $(2\text{S},4\text{S})$ -4-FPGln, **4**, reported in this paper, is a structural analog of glutamine containing a 3-fluoro-propyl substitution group at the C4 position. The mechanisms of uptake for $[^{18}\text{F}](2\text{S},4\text{S})$ -4-FPGln, **4**, are associated with three main amino acid transporters, SLC1A5 (ASCT2), LAT1 (SLC7A5, Na^+ independent), and SNAT (Na^+ /neutral transporter). Based on the inhibition studies, it appears that LAT inhibition was the most prominent, suggesting that LAT may be a preferred transporter for $(2\text{S},4\text{S})$ -4-FPGln, **4**. For $[^{11}\text{C}]\text{Gln}$, **1**, and $(2\text{S},4\text{R})$ -4-FGln, **2**, the most important amino acid transporter appeared to be SLC1A5 (ASCT2).

The in vitro incubation of $[^{18}\text{F}](2\text{S},4\text{S})$ -4-FPGln, **4**, with 9L tumor cells showed a high cell uptake reaching 6% uptake/100 μg of protein at 120 min after incubation. Under the same incubation conditions, the lysate of the 9L cells showed that a significant portion of the $[^{18}\text{F}](2\text{S},4\text{S})$ -4-FPGln, **4**, inside the cells remained intact as the original chemical species (>90% showed no metabolic changes). The $[^3\text{H}]\text{-Gln}$ incubated simultaneously under the same conditions showed substantial incorporation into macromolecules (>90% activity associated with the TCA precipitated fraction). Previously, using the same procedure $[^{11}\text{C}]\text{Gln}$, **1**, and $[^{18}\text{F}](2\text{S},4\text{R})$ -4-FGln, **2**, also displayed very similar incorporations into the macromolecular fraction as that observed for $[^3\text{H}]\text{-Gln}$.^{7,8} The results suggest that $[^{18}\text{F}](2\text{S},4\text{S})$ -4-FPGln, **4**, may be more similar to the neutral LAT preferred amino acid analogs, such as O-(2- $[^{18}\text{F}]$ fluoroethyl)-L-tyrosine (FET).^{33,34} The uptake mechanism may be overlapping that of $[^{18}\text{F}]\text{FACBC}$.^{22,35} All of these

amino acid probes are transported into the cancer cells, without being incorporated into intracellular macromolecules. There are important differences between these seemingly very close glutamine analogs, $[^{18}\text{F}](2\text{S},4\text{R})$ -4-FGln, **2**, and $[^{18}\text{F}](2\text{S},4\text{S})$ -4-FPGln, **4**. Further exploration may be needed to clarify the similarities and differences between these probes. For the development of effective probes for studying glutamine metabolism, one should consider more than simple factors, such as tumor cell uptake and in vivo tumor signal localization. It may also be necessary to consider the subsequent intracellular metabolic processes, or the lack thereof. Compared to the “natural” $[^{11}\text{C}]\text{Gln}$, **1**, fluorine substituted $[^{18}\text{F}](2\text{S},4\text{R})$ -4-FGln, **2**, or $[^{18}\text{F}](2\text{S},4\text{S})$ -4-FPGln, **4**, may always be suspected of having a modified intracellular metabolism. More studies are necessary to characterize these analogs for studying glutamine metabolism in tumors.

The most important difference between $[^{18}\text{F}](2\text{S},4\text{R})$ -4-fluoroglutamic acid (BAY 85–8050) and $[^{18}\text{F}](2\text{S},4\text{S})$ -4-(3-fluoropropyl)glutamic acid (^{18}F -FSPG, or BAY 94–9392) is that ^{18}F -FSPG, displays a slower defluorination rate in vivo. Preliminary human studies have demonstrated that the bone marrow uptake in the vertebral region is relatively low.^{31,32} The same scenario may or may not apply to the second pair of glutamine probes (Figure 10). We have noticed a reduced bone uptake and good tumor uptake in the rats receiving $[^{18}\text{F}](2\text{S},4\text{S})$ -4-FPGln, **4**, as visualized by PET or by a dissection method. Results from both methods suggest a reduced bone uptake (of **4**) in rats as compared to the uptake of $[^{18}\text{F}](2\text{S},4\text{R})$ -4-FGln, **2**.⁸ Loss of fluoride is a constant concern for fluoro-alkyl labeled radiopharmaceuticals. Our observation suggests that defluorination is not an issue for **4**.

In summary, a new glutamine analog, $[^{18}\text{F}](2\text{S},4\text{S})$ -4-FPGln, **4**, has shown tumor specific uptake in vitro and in vivo. However, the tumor uptake and retention mechanisms may be significantly different from other glutamine probes, such as $[^{11}\text{C}]\text{Gln}$, **1**, and $[^{18}\text{F}](2\text{S},4\text{R})$ -4-FGln, **2**.

■ AUTHOR INFORMATION

Corresponding Author

*Email: kungfh@sunmac.spect.upenn.edu. Phone: 215-662-3096. Fax: 215-349-5035.

Author Contributions

§Authors Z.W. and Z.Z. contributed equally to this paper.

Notes

The authors declare no competing financial interest.

ACKNOWLEDGMENTS

The authors thank Dr. Carita Huang for editorial assistance. This work was supported in part by grants from Stand-Up 2 Cancer (SU2C), PA Health Department, and National Institutes of Health (CA-164490; AG-022559; DK-081342).

ABBREVIATIONS

[¹¹C]Gln, L-5-[¹¹C]glutamine, **1**; [¹⁸F](2S,4R)-4-FGln, [¹⁸F](2S,4R)-4-fluoroglutamine, **2**; [¹⁸F](2S,4R)-4-FPGln, [¹⁸F](2S,4R)-4-(3-fluoropropyl)glutamine, **3**; [¹⁸F](2S,4S)-4-FPGln, [¹⁸F](2S,4S)-4-(3-fluoropropyl)glutamine, **4**; ASC, alanine-serine-cysteine preferring amino acid transporter system; ASCT2, system ASC transporter subtype 2; BCH, 2-amino-bicyclo[2.2.1]heptane-2-carboxylic acid; MeAIB, N-methyl- α -aminoisobutyric acid; FACBC, 3-[¹⁸F]fluoro-cyclobutyl-1-carboxylic acid; FC, flash chromatography; FDG, 2-[¹⁸F]fluoro-2-deoxy-D-glucose; FET, O-(2-[¹⁸F]fluoroethyl)-L-tyrosine; [³H]Gln, L-[3,4-³H(N)]-glutamine; HPLC, High-performance liquid chromatography; HRMS, High-resolution mass spectrometry; MeAIB, N-methyl- α -aminoisobutyric acid; TCA, trichloroacetic acid; TFA, trifluoroacetic acid; PET, positron emission tomography

REFERENCES

(1) Koppenol, W. H.; Bounds, P. L.; Dang, C. V. Otto Warburg's contributions to current concepts of cancer metabolism. *Nat. Rev. Cancer* **2011**, *11*, 325–37.

(2) Jadvar, H.; Alavi, A.; Gambhir, S. S. ¹⁸F-FDG uptake in lung, breast, and colon cancers: molecular biology correlates and disease characterization. *J. Nucl. Med.* **2009**, *50*, 1820–7.

(3) Wise, D. R.; Thompson, C. B. Glutamine addiction: a new therapeutic target in cancer. *Trends Biochem. Sci.* **2010**, *35*, 427–33.

(4) Wise, D. R.; Ward, P. S.; Shay, J. E.; Cross, J. R.; Gruber, J. J.; Sachdeva, U. M.; Platt, J. M.; Dematteo, R. G.; Simon, M. C.; Thompson, C. B. Hypoxia promotes isocitrate dehydrogenase-dependent carboxylation of alpha-ketoglutarate to citrate to support cell growth and viability. *Proc. Natl. Acad. Sci. U. S. A.* **2011**, *108*, 19611–6.

(5) Le, A.; Lane, A. N.; Hamaker, M.; Bose, S.; Gouw, A.; Barbi, J.; Tsukamoto, T.; Rojas, C. J.; Slusher, B. S.; Zhang, H.; Zimmerman, L. J.; Liebler, D. C.; Slebos, R. J.; Lorkiewicz, P. K.; Higashi, R. M.; Fan, T. W.; Dang, C. V. Glucose-independent glutamine metabolism via TCA cycling for proliferation and survival in B cells. *Cell Metab.* **2012**, *15*, 110–21.

(6) Daye, D.; Wellen, K. E. Metabolic reprogramming in cancer: Unraveling the role of glutamine in tumorigenesis. *Semin. Cell Dev. Biol.* **2012**, *23*, 362–9.

(7) Qu, W.; Oya, S.; Lieberman, B. P.; Ploessl, K.; Wang, L.; Wise, D. R.; Divgi, C. D.; Chodosh, L. A.; Thompson, C. B.; Kung, H. F. Preparation and Characterization of L-[⁵⁻¹¹C]-Glutamine for Metabolic Imaging of Tumors. *J. Nucl. Med.* **2012**, *53*, 98–105.

(8) Lieberman, B. P.; Ploessl, K.; Wang, L.; Qu, W.; Zha, Z.; Wise, D. R.; Chodosh, L. A.; Belka, G.; Thompson, C. B.; Kung, H. F. PET imaging of glutaminolysis in tumors by ¹⁸F-(2S,4R)-4-fluoroglutamine. *J. Nucl. Med.* **2011**, *52*, 1947–55.

(9) Qu, W.; Zha, Z.; Ploessl, K.; Lieberman, B. P.; Zhu, L.; Wise, D. R.; Thompson, C. B.; Kung, H. F. Synthesis of optically pure 4-fluoroglutamines as potential metabolic imaging agents for tumors. *J. Am. Chem. Soc.* **2011**, *133*, 1122–33.

(10) Dang, C. V.; Hamaker, M.; Sun, P.; Le, A.; Gao, P. Therapeutic targeting of cancer cell metabolism. *J. Mol. Med.* **2011**, *89*, 205–12.

(11) Fan, X.; Ross, D. D.; Arakawa, H.; Ganapathy, V.; Tamai, I.; Nakanishi, T. Impact of system L amino acid transporter 1 (LAT1) on

proliferation of human ovarian cancer cells: a possible target for combination therapy with anti-proliferative aminopeptidase inhibitors. *Biochem. Pharmacol.* **2010**, *80*, 811–8.

(12) Esslinger, C. S.; Agarwal, S.; Gerdes, J.; Wilson, P. A.; Davis, E. S.; Awes, A. N.; O'Brien, E.; Mavencamp, T.; Koch, H. P.; Poulsen, D. J.; Rhoderick, J. F.; Chamberlin, A. R.; Kavanaugh, M. P.; Bridges, R. J. The substituted aspartate analogue L-beta-threo-benzyl-aspartate preferentially inhibits the neuronal excitatory amino acid transporter EAAT3. *Neuropharmacology* **2005**, *49*, 850–61.

(13) Bridges, R. J.; Esslinger, C. S. The excitatory amino acid transporters: pharmacological insights on substrate and inhibitor specificity of the EAAT subtypes. *Pharmacol. Ther.* **2005**, *107*, 271–85.

(14) Hanessian, S.; Margarita, R.; Hall, A.; Luo, X. 1,2-Asymmetric induction in dianionic allylation reactions of amino acid derivatives - synthesis of functionally useful, enantiopure aspartates and constrained scaffolds. *Tetrahedron Lett.* **1998**, *39*, 5883–5886.

(15) Lee, T. S.; Ahn, S. H.; Moon, B. S.; Chun, K. S.; Kang, J. H.; Cheon, G. J.; Choi, C. W.; Lim, S. M. Comparison of ¹⁸F-FDG, ¹⁸F-FET and ¹⁸F-FLT for differentiation between tumor and inflammation in rats. *Nucl. Med. Biol.* **2009**, *36*, 681–6.

(16) Bungard, C. I.; McGivan, J. D. Glutamine availability up-regulates expression of the amino acid transporter protein ASCT2 in HepG2 cells and stimulates the ASCT2 promoter. *Biochem. J.* **2004**, *382*, 27–32.

(17) Bungard, C. I.; McGivan, J. D. Identification of the promoter elements involved in the stimulation of ASCT2 expression by glutamine availability in HepG2 cells and the probable involvement of FXR/RXR dimers. *Arch. Biochem. Biophys.* **2005**, *443*, 53–9.

(18) McGivan, J. D.; Bungard, C. I. The transport of glutamine into mammalian cells. *Front. Biosci.* **2007**, *12*, 874–82.

(19) Plathow, C.; Weber, W. A. Tumor cell metabolism imaging. *J. Nucl. Med.* **2008**, *49* (Suppl 2), 43S–63S.

(20) McConathy, J.; Yu, W.; Jarkas, N.; Seo, W.; Schuster, D. M.; Goodman, M. M. Radiohalogenated nonnatural amino acids as PET and SPECT tumor imaging agents. *Med. Res. Rev.* **2012**, *32*, 868–905.

(21) Huang, C.; McConathy, J. Radiolabeled amino acids for oncologic imaging. *J. Nucl. Med.* **2013**, *54*, 1007–10.

(22) Oka, S.; Okudaira, H.; Ono, M.; Schuster, D. M.; Goodman, M. M.; Kawai, K.; Shirakami, Y. Differences in Transport Mechanisms of trans-1-Amino-3-[¹⁸F]Fluorocyclobutanecarboxylic Acid in Inflammation, Prostate Cancer, and Glioma Cells: Comparison with L-[Methyl-C]Methionine and 2-Deoxy-2-[¹⁸F]Fluoro-D-Glucose. *Mol. Imaging Biol.* **2014**, *16*, 322–329.

(23) Okudaira, H.; Nakanishi, T.; Oka, S.; Kobayashi, M.; Tamagami, H.; Schuster, D. M.; Goodman, M. M.; Shirakami, Y.; Tamai, I.; Kawai, K. Kinetic analyses of trans-1-amino-3-[¹⁸F]-fluorocyclobutanecarboxylic acid transport in *Xenopus laevis* oocytes expressing human ASCT2 and SNAT2. *Nucl. Med. Biol.* **2013**, *40*, 670–5.

(24) Sorensen, J.; Owenius, R.; Lax, M.; Johansson, S. Regional distribution and kinetics of [¹⁸F]fluciclovine (anti-[¹⁸F]FACBC), a tracer of amino acid transport, in subjects with primary prostate cancer. *Eur. J. Nucl. Med. Mol. Imaging* **2013**, *40*, 394–402.

(25) Turkbey, B.; Mena, E.; Shih, J.; Pinto, P. A.; Merino, M. J.; Lindenberg, M. L.; Bernardo, M.; McKinney, Y. L.; Adler, S.; Owenius, R.; Choyke, P. L.; Kurdziel, K. A. Localized Prostate Cancer Detection with ¹⁸F FACBC PET/CT: Comparison with MR Imaging and Histopathologic Analysis. *Radiology* **2014**, *270*, 849–56.

(26) Okudaira, H.; Shikano, N.; Nishii, R.; Miyagi, T.; Yoshimoto, M.; Kobayashi, M.; Ohe, K.; Nakanishi, T.; Tamai, I.; Namiki, M.; Kawai, K. Putative Transport Mechanism and Intracellular Fate of Trans-1-Amino-3-¹⁸F-Fluorocyclobutanecarboxylic Acid in Human Prostate Cancer. *J. Nucl. Med.* **2011**, *52*, 822–9.

(27) Oka, S.; Okudaira, H.; Yoshida, Y.; Schuster, D. M.; Goodman, M. M.; Shirakami, Y. Transport mechanisms of trans-1-amino-3-fluoro[¹⁻¹⁴C]cyclobutanecarboxylic acid in prostate cancer cells. *Nucl. Med. Biol.* **2012**, *39*, 109–119.

(28) Schuster, D. M.; Savir-Baruch, B.; Nieh, P. T.; Master, V. A.; Halkar, R. K.; Rossi, P. J.; Lewis, M. M.; Nye, J. A.; Yu, W.; Bowman,

F. D.; Goodman, M. M. Detection of recurrent prostate carcinoma with anti-1-amino-3-¹⁸F-fluorocyclobutane-1-carboxylic acid PET/CT and ¹¹¹In-capromab pendetide SPECT/CT. *Radiology* **2011**, *259*, 852–61.

(29) Krasikova, R. N.; Kuznetsova, O. F.; Fedorova, O. S.; Belokon, Y. N.; Maleev, V. I.; Mu, L.; Ametamey, S.; Schubiger, P. A.; Friebe, M.; Berndt, M.; Koglin, N.; Mueller, A.; Graham, K.; Lehmann, L.; Dinkelborg, L. M. 4-[¹⁸F]Fluoroglutamic Acid (BAY 85–8050), a New Amino Acid Radiotracer for PET Imaging of Tumors: Synthesis and in Vitro Characterization. *J. Med. Chem.* **2011**, *54*, 406–410.

(30) Koglin, N.; Mueller, A.; Berndt, M.; Schmitt-Willich, H.; Toschi, L.; Stephens, A. W.; Gekeler, V.; Friebe, M.; Dinkelborg, L. M. Specific PET imaging of xC⁻ transporter activity using a ¹⁸F-labeled glutamate derivative reveals a dominant pathway in tumor metabolism. *Clin. Cancer Res.* **2011**, *17*, 6000–6011.

(31) Baek, S.; Choi, C. M.; Ahn, S. H.; Lee, J. W.; Gong, G.; Ryu, J. S.; Oh, S. J.; Bacher-Stier, C.; Fels, L.; Koglin, N.; Hultsch, C.; Schatz, C. A.; Dinkelborg, L. M.; Mittra, E. S.; Gambhir, S. S.; Moon, D. H. Exploratory clinical trial of (4S)-4-(3-[¹⁸F]fluoropropyl)-L-glutamate for imaging xC⁻ transporter using positron emission tomography in patients with non-small cell lung or breast cancer. *Clin. Cancer Res.* **2012**, *18*, 5427–37.

(32) Baek, S.; Mueller, A.; Lim, Y. S.; Lee, H. C.; Lee, Y. J.; Gong, G.; Kim, J. S.; Ryu, J. S.; Oh, S. J.; Lee, S. J.; Bacher-Stier, C.; Fels, L.; Koglin, N.; Schatz, C. A.; Dinkelborg, L. M.; Moon, D. H. (4S)-4-(3-[¹⁸F]fluoropropyl)-L-glutamate for imaging of xC transporter activity in hepatocellular carcinoma using PET: preclinical and exploratory clinical studies. *J. Nucl. Med.* **2013**, *54*, 117–23.

(33) Wang, L.; Qu, W.; Lieberman, B. P.; Plossl, K.; Kung, H. F. Synthesis, uptake mechanism characterization and biological evaluation of ¹⁸F labeled fluoroalkyl phenylalanine analogs as potential PET imaging agents. *Nucl. Med. Biol.* **2011**, *38*, 53–62.

(34) Langen, K. J.; Hamacher, K.; Weckesser, M.; Floeth, F.; Stoffels, G.; Bauer, D.; Coenen, H. H.; Pauleit, D. O-(2-[¹⁸F]fluoroethyl)-L-tyrosine: uptake mechanisms and clinical applications. *Nucl. Med. Biol.* **2006**, *33*, 287–94.

(35) Ono, M.; Oka, S.; Okudaira, H.; Schuster, D. M.; Goodman, M. M.; Kawai, K.; Shirakami, Y. Comparative evaluation of transport mechanisms of trans-1-amino-3-[¹⁸F]fluorocyclobutanecarboxylic acid and L-[methyl-¹¹C]methionine in human glioma cell lines. *Brain Res.* **2013**, *1535*, 24–37.